

the ECG features presented here to locate subjects in wide populations, such as health examinations, who are at risk.

### Acknowledgments

The authors thank Kahaku Emoto, Seiichi Fujisaki, and Tatsumi Uchiyama (GE Yokokawa Medical System Co) for their technical assistance.

### Disclosures

No conflicts to disclose.

### References

- Brugada P, Brugada J. Right bundle branch block, persistent ST segment elevation and sudden cardiac death: A distinct clinical and electrocardiographic syndrome: A multicenter report. *J Am Coll Cardiol* 1992; **20**: 1391–1396.
- Antzelevitch C, Brugada P, Borggrefe M, Brugada J, Brugada R, Corrado D, et al. Brugada syndrome: Report of the second consensus conference: Endorsed by the heart rhythm society and the european heart rhythm association. *Circulation* 2005; **111**: 659–670.
- Miyasaka Y, Tsuji H, Yamada K, Tokunaga S, Saito D, Imuro Y, et al. Prevalence and mortality of the Brugada-type electrocardiogram in one city in japan. *J Am Coll Cardiol* 2001; **38**: 771–774.
- Matsuo K, Akahoshi M, Nakashima E, Suyama A, Seto S, Hayano M, et al. The prevalence, incidence and prognostic value of the Brugada-type electrocardiogram: A population-based study of four decades. *J Am Coll Cardiol* 2001; **38**: 765–770.
- Brugada J, Brugada R, Antzelevitch C, Towbin J, Nademanee K, Brugada P. Long-term follow-up of individuals with the electrocardiographic pattern of right bundle-branch block and ST-segment elevation in precordial leads V1 to V3. *Circulation* 2002; **105**: 73–78.
- Priori SG, Napolitano C, Gasparini M, Pappone C, Della Bella P, Giordano U, et al. Natural history of Brugada syndrome: Insights for risk stratification and management. *Circulation* 2002; **105**: 1342–1347.
- Eckardt L, Probst V, Smits JP, Bahr ES, Wolpert C, Schimpf R, et al. Long-term prognosis of individuals with right precordial ST-segment-elevation brugada syndrome. *Circulation* 2005; **111**: 257–263.
- Brugada P, Brugada R, Brugada J. Should patients with an asymptomatic Brugada electrocardiogram undergo pharmacological and electrophysiological testing? *Circulation* 2005; **112**: 279–292; discussion 279–292.
- Priori SG, Napolitano C. Should patients with an asymptomatic Brugada electrocardiogram undergo pharmacological and electrophysiological testing? *Circulation* 2005; **112**: 279–292; discussion 279–292.
- Chen Q, Kirsch GE, Zhang D, Brugada R, Brugada J, Brugada P, et al. Genetic basis and molecular mechanism for idiopathic ventricular fibrillation. *Nature* 1998; **392**: 293–296.
- Makiyama T, Akao M, Shizuta S, Doi T, Nishiyama K, Oka Y, et al. A novel scn5a gain-of-function mutation M1875T associated with familial atrial fibrillation. *J Am Coll Cardiol* 2008; **52**: 1326–1334.
- Kawamura M, Ozawa T, Yao T, Ashihara T, Sugimoto Y, Yagi T, et al. Dynamic change in ST-segment and spontaneous occurrence of ventricular fibrillation in Brugada syndrome with a novel non-sense mutation in the SCN5A gene during long-term follow-up. *Circ J* 2009; **73**: 584–588.
- Yan GX, Antzelevitch C. Cellular basis for the Brugada syndrome and other mechanisms of arrhythmogenesis associated with ST-segment elevation. *Circulation* 1999; **100**: 1660–1666.
- Nagase S, Kusano KF, Morita H, Nishii N, Banba K, Watanabe A, et al. Longer repolarization in the epicardium at the right ventricular outflow tract causes type 1 electrocardiogram in patients with Brugada syndrome. *J Am Coll Cardiol* 2008; **51**: 1154–1161.
- Ashino S, Watanabe I, Kofune M, Nagashima K, Ohkubo K, Okumura Y, et al. Abnormal action potential duration restitution property in the right ventricular outflow tract in Brugada syndrome. *Circ J* 2010; **74**: 664–670.
- Kanda M, Shimizu W, Matsuo K, Nagaya N, Taguchi A, Suyama K, et al. Electrophysiologic characteristics and implications of induced ventricular fibrillation in symptomatic patients with Brugada syndrome. *J Am Coll Cardiol* 2002; **39**: 1799–1805.
- Morita H, Kusano-Fukushima K, Nagase S, Fujimoto Y, Hisamatsu K, Fujio H, et al. Atrial fibrillation and atrial vulnerability in patients with Brugada syndrome. *J Am Coll Cardiol* 2002; **40**: 1437–1444.
- Kusano KF, Taniyama M, Nakamura K, Miura D, Banba K, Nagase S, et al. Atrial fibrillation in patients with Brugada syndrome relationships of gene mutation, electrophysiology, and clinical backgrounds. *J Am Coll Cardiol* 2008; **51**: 1169–1175.
- Yamada T, Watanabe I, Okumura Y, Takagi Y, Okubo K, Hashimoto K, et al. Atrial electrophysiological abnormality in patients with Brugada syndrome assessed by P-wave signal-averaged ECG and programmed atrial stimulation. *Circ J* 2006; **70**: 1574–1579.
- Hayashi H, Sumiyoshi M, Yasuda M, Komatsu K, Sekita G, Kawano Y, et al. Prevalence of the Brugada-type electrocardiogram and incidence of Brugada syndrome in patients with sick sinus syndrome. *Circ J* 2010; **74**: 271–277.
- Brugada J, Brugada R, Brugada P. Right bundle-branch block and ST-segment elevation in leads V1 through V3: A marker for sudden death in patients without demonstrable structural heart disease. *Circulation* 1998; **97**: 457–460.

### Supplemental Files

#### Supplemental File 1

Figure S1. 12-lead ECG of a 49-year-old man who was diagnosed with Brugada syndrome.

Figure S2. 12-lead ECG of a 55-year-old man who was undiagnosed with Brugada syndrome.

Table S1. Comparison of ECG Variables Between Patients With and Without ICD Intervention in the BS Diagnosis Group

Please find supplemental file(s);  
<http://dx.doi.org/10.1253/circj.CJ-10-0903>

## Remission of Abnormal Conduction and Repolarization in the Right Ventricle After Chemotherapy in Patients With Anterior Mediastinal Tumor

AKASHI MIYAMOTO, M.D., HIDEKI HAYASHI, M.D., PH.D., MAKOTO ITO, M.D., PH.D.,  
and MINORU HORIE, M.D., PH.D.

From the Department of Cardiovascular and Respiratory Medicine, Shiga University of Medical Science, Shiga, Japan

A 22-year-old man with no significant past medical history presented with dry cough that lasted for a couple of months. The patient denied accompanying shortness of breath, palpitation, edema, high fever, or syncope. He had no family history of sudden death. On examination, he was afebrile with a blood pressure of 106/63 mm Hg, pulse rate of 88 beats/min, and normal oxygen saturation. His heart sound was normal without a pericardial rub. ECG (Fig. 1A) displayed a terminal r wave (arrow a) and ST-segment elevation (arrow b) followed by negative deflection of T wave (arrow c) in lead V<sub>1</sub>. Chest computed tomography (Fig. 1A) revealed the existence of demarcated tumor in the anterior mediastinal space that attached to the pericardium in front of the right atrium and ventricle. The tumor encompassed the right ventricular outflow tract (arrow) but did not show invasion into the intrapericardial space. The tumor was histologically diagnosed with the large B cell lymphoma from a specimen obtained by needle biopsy. He started to undergo chemotherapy including cyclophosphamide, vincristine, doxorubicin, rituximab, and prednisolone. Two months after the chemotherapy, chest computed tomography confirmed that the lymphoma size

was reduced, which was almost invisible (Fig. 1B). At that time, ECG showed the disappearance of a late r wave and ST-segment elevation in lead V<sub>1</sub> (Fig. 1B). These findings indicate that coinciding with the shrinkage of anterior mediastinal tumor, conduction disturbance, and abnormal repolarization in the right ventricle were resolved. No life-threatening arrhythmic event occurred during the follow-up.

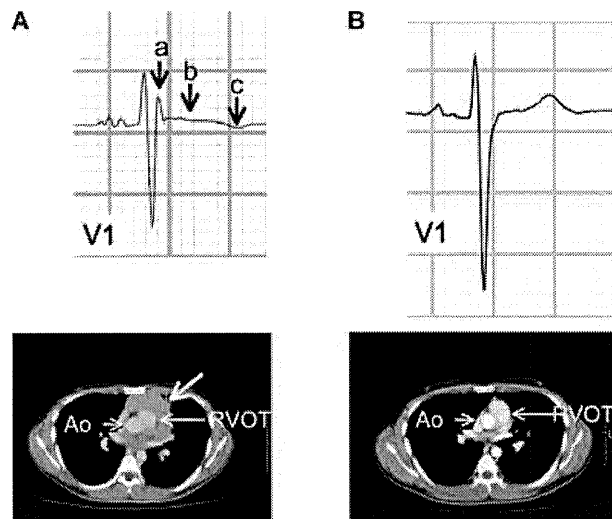


**Figure 1.** A and B: ECG recording in lead V<sub>1</sub> and contrast-enhanced computed tomography scan before and after chemotherapy, respectively. Ao = Aorta; RVOT = right ventricular outflow tract.

J Cardiovasc Electrophysiol, Vol. 22, p. 350, March 2011.

No disclosures.

Address for correspondence: Hideki Hayashi, M.D., Ph.D., Department of Cardiovascular and Respiratory Medicine, Shiga University of Medical Science, Otsu, Shiga 520-2192, Japan. Fax: 81-77-543-5839; E-mail: hayashih@belle.shiga-med.ac.jp

doi: 10.1111/j.1540-8167.2010.01898.x

## Informatic and Functional Approaches to Identifying a Regulatory Region for the Cardiac Sodium Channel

Thomas C. Atack, Dina Myers Stroud, Hiroshi Watanabe, Tao Yang, Lynn Hall, Susan B. Hipkens, John S. Lowe, Brenda Leake, Mark A. Magnuson, Ping Yang, Dan M. Roden

**Rationale:** Although multiple lines of evidence suggest that variable expression of the cardiac sodium channel gene *SCN5A* plays a role in susceptibility to arrhythmia, little is known about its transcriptional regulation.

**Objective:** We used *in silico* and *in vitro* experiments to identify possible noncoding sequences important for transcriptional regulation of *SCN5A*. The results were extended to mice in which a putative regulatory region was deleted.

**Methods and Results:** We identified 92 noncoding regions highly conserved (>70%) between human and mouse *SCN5A* orthologs. Three conserved noncoding sequences (CNS) showed significant (>5-fold) activity in luciferase assays. Further *in vitro* studies indicated one, CNS28 in intron 1, as a potential regulatory region. Using recombinase-mediated cassette exchange (RMCE), we generated mice in which a 435-base pair region encompassing CNS28 was removed. Animals homozygous for the deletion showed significant increases in *SCN5A* transcripts,  $\text{Na}_v1.5$  protein abundance, and sodium current measured in isolated ventricular myocytes. ECGs revealed a significantly shorter QRS ( $10.7 \pm 0.2$  ms in controls versus  $9.7 \pm 0.2$  ms in knockouts), indicating more rapid ventricular conduction. *In vitro* analysis of CNS28 identified a short 3' segment within this region required for regulatory activity and including an E-box motif. Deletion of this segment reduced reporter activity to  $3.6\% \pm 0.3\%$  of baseline in CHO cells and  $16\% \pm 3\%$  in myocytes (both  $P < 0.05$ ), and mutation of individual sites in the E-box restored activity to  $62\% \pm 4\%$  and  $57\% \pm 2\%$  of baseline in CHO cells and myocytes, respectively (both  $P < 0.05$ ).

**Conclusions:** These findings establish that regulation of cardiac sodium channel expression modulates channel function *in vivo*, and identify a noncoding region underlying this regulation. (*Circ Res.* 2011;109:38-46.)

**Key Words:** gene expression regulation ■ sodium channels ■ mice ■ transgenic

Normal function of the sodium channel encoded by *SCN5A* is critical to initiation of the action potential and its propagation in atrium and ventricle.<sup>1</sup> Mutations that decrease sodium current ( $I_{\text{Na}}$ ) by disrupting channel processing or function cause a series of overlapping human arrhythmia syndromes, including Brugada Syndrome and conduction system disease.<sup>1,2</sup> In subjects of Asian ancestry, we have described a common variant in the *SCN5A* core promoter that modulates the duration of the QRS interval, an index of ventricular conduction, in normal subjects.<sup>3</sup> In addition, the promoter variant appeared to modulate the extent to which drug challenge prolonged QRS in patients with the Brugada Syndrome. Notably, QRS prolongation is a hallmark of sodium channel block by drugs, and sodium channel blockers are well recognized to have proarrhythmic potential.<sup>4</sup>

Taken together, these findings implicate variability in *SCN5A* expression as a mechanism underlying arrhythmia susceptibility in the whole heart. To date, few studies have addressed mechanisms underlying transcriptional control of *SCN5A* expression. We have previously identified the core promoter of human *SCN5A* and common polymorphisms in that region.<sup>5,6</sup> Others have reported that transgenic cardiac expression of the putative repressor Snail led to decreased  $I_{\text{Na}}$  and dilated cardiomyopathy; further experiments suggested that *Scn5a* is a Snail target.<sup>7</sup> Snail is zinc-finger transcription factor known to target E-box motifs.<sup>8</sup> Shang and Dudley reported multiple alternate 5'-splice variants of the murine sodium channel ortholog; these were developmentally regulated, and both enhancer and repressor regulatory elements and an alternate promoter were identified.<sup>9</sup>

Original received October 28, 2010; revision received April 8, 2011; accepted May 4, 2011. In April 2011, the average time from submission to first decision for all original research papers submitted to *Circulation Research* was 15 days.

From the Department of Medicine (T.C.A., D.M.S., H.W., T.Y., L.H., J.S.L., B.L., P.Y.), Molecular Physiology (S.B.H., M.A.M.), and Biophysics (S.B.H., M.A.M.) and the Department of Pharmacology (D.M.R.), Vanderbilt University School of Medicine, Nashville, Tennessee.

Hiroshi Watanabe is currently affiliated with the Division of Cardiology, Niigata University Graduate School of Medical and Dental Sciences, Niigata, Japan.

Correspondence to Dan M. Roden, MD, Director, Oates Institute for Experimental Therapeutics, Assistant Vice-Chancellor for Personalized Medicine, Vanderbilt University School of Medicine, 2215B Garland Avenue, 1285 MRBIV Light Hall, Nashville, TN 37232-0575. E-mail dan.roden@vanderbilt.edu

© 2011 American Heart Association, Inc.

*Circulation Research* is available at <http://circres.ahajournals.org>

DOI: 10.1161/CIRCRESAHA.110.235630

**Table. PCR and Mutagenesis Primers**

Primer	Sequence
CNS28 <sup>-/-</sup> mouse genotyping	
F	ATGGAGGCCAAAGGTCAGCTTGACG
R	TGAGCATGTTGAAGAGCGAGTGAACAG
Human CNS28 for pGL3- <i>SCN5A</i> promoter	
F_ <i>Sall</i>	TGAGGTACCGTTCTGAATCTTTGAGGCC
R_ <i>BamHI</i>	TCAAGATCTGATTCTAAAGACGGGAAATG
Alternate mouse promoter deletion constructs	
DC0-F	TGAGGTACCCCTTATAGGGTCACTAATGACATGCC
DC1-F	TGAGGTACCCCTTGGCTGACAGGAAGAGAGTGTG
DC2-F	TGAGGTACCGTGGTAATTAGCGGTGCAGCCTCCT
DC3-F	TGAGGTACCGTCTGAATCTTTGAGGCCACCAGG
DC4-F	TGAGGTACCGTCTAGCTAGGGACGGTGTCTGC
DC-R	TCAAGATCTCACAGGCTCTCCTCAGGCTGCCT
E-box mutagenesis	
F	ACGTCACACACTTAAGCCTGTTGGAAGTCC
R	GGACTCCAACAGGCTTAAGTGTGTGACGT

In this report, we first identified short sequences highly conserved between mouse and human. Further studies implicated one of these conserved noncoding sequences (CNS), designated CNS28 and located  $\approx 1.3$  kb upstream of exon 2, as a potential regulator of channel expression. To further test this hypothesis in vivo, we determined the electrophysiological properties of mice in which the CNS28 region was deleted. We find that the absence of CNS28 results in striking increases in sodium channel expression in the intact heart, with attendant increased sodium current and conduction. Additional experiments in heterologous cells and cardiomyocytes implicate the loss of an E-box binding site as responsible for this increase in sodium channel expression.

## Methods

Details for each method are presented in the Online Supplement available at <http://circres.ahajournals.org>.

### Identification of Potential Regulatory Regions

To identify CNS elements, we compared the human *SCN5A* locus with its mouse ortholog using the VISTA Genome Browser (<http://pipeline.lbl.gov/cgi-bin/gateway2>).<sup>10,11</sup> Each of 92 CNS elements identified was then PCR amplified and assayed for activity as described below and in the On-Line Supplement. Those showing  $>5$ -fold increase in reporter activity in luciferase assays were then analyzed for potential muscle-specific transcriptional regulatory modules using the M-SCAN algorithm (<http://www.cisreg.ca/cgi-bin/mscan/MSCAN>).<sup>12,13</sup> For identification of potential repressive transcription factors in CNS28, we used rVista (<http://rvista.dcode.org/>) to compare human and mouse sequences for conserved transcription factor-binding sites.<sup>14,15</sup>

### Reporter Constructs

Reporter constructs measuring the activity of all 92 CNS constructs (Online Table I), human CNS28 with the full-length human *SCN5A* promoter (Table), and deletion analysis of the alternate mouse *Scn5a*

### Nonstandard Abbreviations and Acronyms

<b>CHO</b>	Chinese hamster ovary
<b>CNS</b>	conserved noncoding sequence
<b>ECG</b>	electrocardiogram
<b>H</b>	humanized <i>SCN5A</i> allele
<b>Na<sub>v</sub>1.5</b>	voltage-gated cardiac sodium channel
<b>RMCE</b>	recombinase mediated cassette exchange

promoter (Table) were generated by cloning PCR fragments into the pGL3-promoter or pGL3-basic vectors (Promega). Mutagenesis of the DC3 deletion fragment was performed using the QuickChange XL II kit (Stratagene) using the primers listed in Table. Reporter assays were conducted as previously described in CHO cells<sup>5,6</sup> and in cardiomyocytes<sup>5,6,16</sup> isolated from 1- to 2-day-old mice.

### Generation of CNS28<sup>-/-</sup> Mice

We used mouse embryonic stem (ES) cells in which a region of the *Scn5a* gene was modified to allow recombinase-mediated cassette exchange (RMCE)<sup>17,18</sup> to be used to easily generate animals containing allelic variants of human sodium channels under control of *Scn5a* regulatory sequences. Using this approach, we previously generated H/H mice in which the targeted region was replaced by the human *SCN5A* full-length cDNA.<sup>19</sup> For the present experiments, we modified the original H exchange construct to delete bases 1720 to 2154 (that encompass the CNS28 region), and then performed RMCE as previously described to generate CNS28<sup>+/-</sup> animals.<sup>19</sup> After removal of the hygromycin resistance cassette by breeding to a FlpE-expressing line, mice were then interbred to generate CNS28<sup>-/-</sup> animals. Experiments began after 3 backcrosses using littermate H/H mice as controls. All experiments performed on mice were approved by the institutional animal care and use committee.

### Quantitative Real-Time RT-PCR

Total mRNA from adult mice atria or ventricles was isolated using the TRIzol method (Invitrogen) and cDNA was prepared using the Transcriptor First-Strand cDNA Synthesis kit (Roche). Quantitative real-time RT-PCR (qPCR) on *SCN5A* was performed with TaqMan probes targeting human *SCN5A* (Hs00165693\_m1) using beta actin (Mm00607939\_s1) as a reference gene. The qPCR targeting mouse *Scn1b* was performed using TaqMan probe (Mm00441210\_m1) with *Hprt1* (Mm00446968\_m1) as the reference gene. Analysis was performed using SDS 2.2.2 software (Applied Biosystems).

### Western Blotting

Western blotting protocol and semiquantitative protein analysis are described in the Online Supplement.

### ECG (ECG) Recordings and Lidocaine Challenge

ECGs and drug challenges were recorded as previously described.<sup>20</sup>

### Isolation of Mouse Ventricular Cardiomyocytes and Sodium Current Recordings

Adult H/H and CNS28<sup>-/-</sup> mouse cardiac ventricular myocytes were isolated by a modified collagenase/protease method,<sup>21</sup> and sodium current studied as previously described.<sup>19</sup> Protocols and data analysis are presented in the Online Supplement.

### Echocardiogram

Transthoracic echocardiograms were performed on resting conscious mice at the murine cardiovascular core, Vanderbilt University, as previously described.<sup>22</sup> Signals were acquired using a 15-MHz transducer (Sonos 5500 system, Agilent) and analyzed by a sonographer who was blind to the genotype.

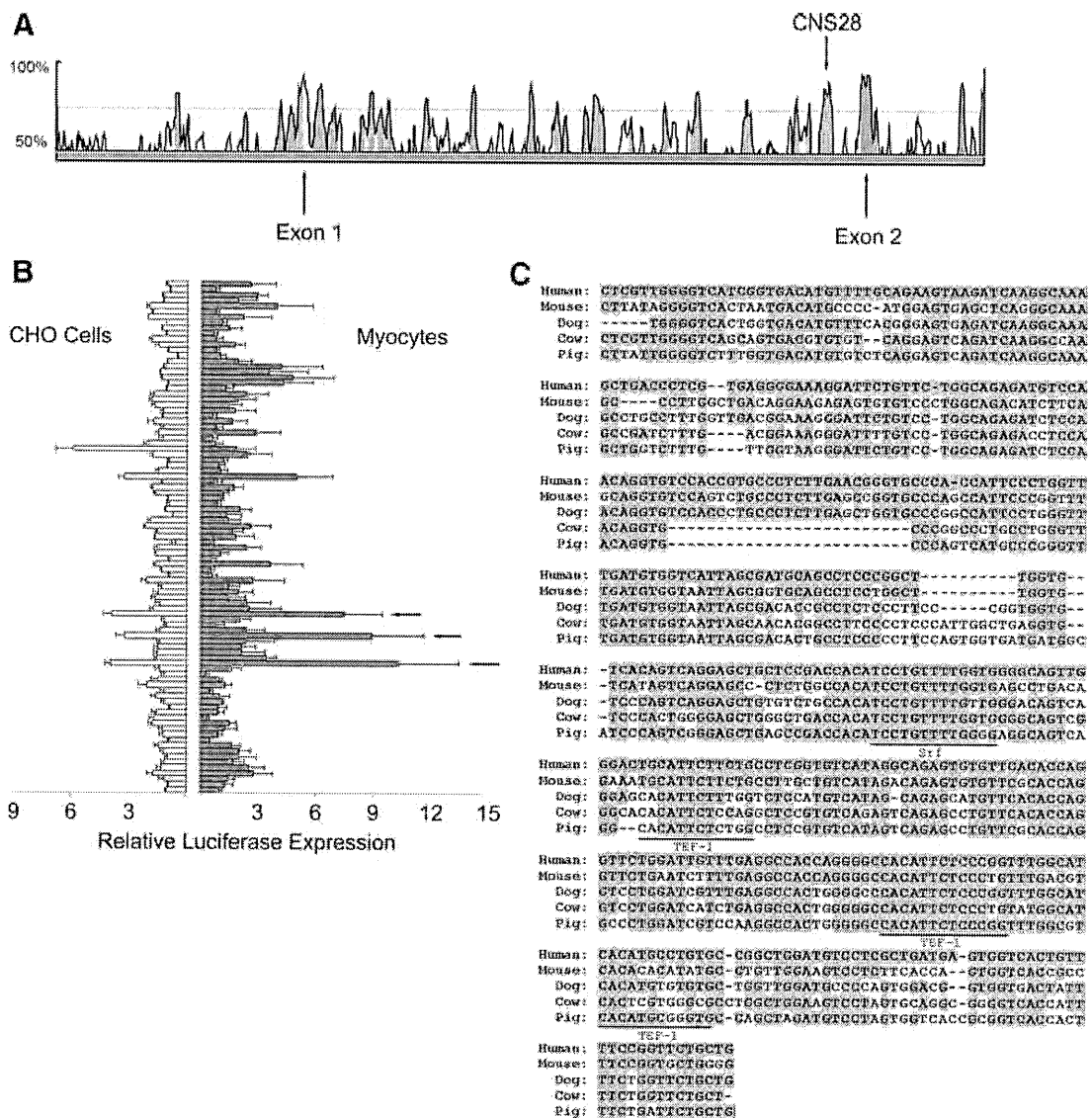


**Figure 1. Identification of CNS28.** **A**, A portion of the VISTA human-to-mouse sequence comparison for *SCN5A* with the locations of Exon 1, Exon 2, and CNS28 marked. The peaks show regions of high conservation across species. Peaks that are shaded satisfy the CNS selection criteria of 70% identity between sequences. **B**, Initial luciferase experiments of all 92 CNS constructs in CHO cells and myocytes with CNS23, CNS28, and CNS32 marked by arrows. **C**, Human CNS28 aligned with mouse, dog, cow, and pig orthologs with the TEF-1 and SRF sites suggested by MSCAN marked.

**Data Analysis**

Results are presented as mean±SE, and statistical comparisons were made using the unpaired Student *t* test. A value of *P*<0.05 was considered statistically significant.

**Results**

**Conserved Nucleotide Sequences**

In order to identify genomic elements that may play a role in the transcriptional regulation of *SCN5A*, we compared human and mouse *SCN5A* sequences to identify conserved regions. Using the genomic sequence comparison program VISTA, we identified 92 CNS elements 77 to 446 base pairs (bp) long with >70% nucleotide identity between the human locus and its mouse ortholog. We identified 12 out of 92 CNS elements in the 47.7-kb 5' upstream region between *SCN5A* exon 1 and the terminal exon of *SCN10A* gene, which is just upstream,

and 15 of 92 CNS elements were identified in the 26.4-kb 3' downstream region between the terminal exon (exon 28) of *SCN5A* and the exon 1 of the downstream gene *ENDOGL1*. The highest density was in intron 1, where 23 CNS elements were contained in 16 kb (Figure 1A). Ten introns contained no CNS elements.

We tested the effect of each CNS on the SV40 promoter driving luciferase both in Chinese hamster ovary (CHO) cells and cardiomyocytes. There were 3 elements, CNS23, CNS28 and CNS32, that demonstrated a >5-fold increase in reporter activity (Figure 1B). The MSCAN analysis, which we used to identify potential functionally important clusters of muscle-specific transcription factors, designated 3 tandem TEF-1 (transcriptional enhancer factor 1) sites and an SRF (serum response factor) recognition site in CNS28 (Figure 1C), and no elements in the other 2. There was a high degree of

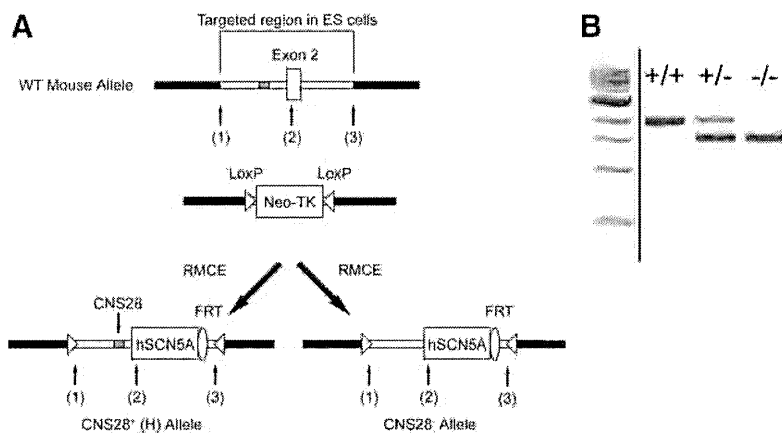


**Figure 2. Generation of *CNS28*<sup>-/-</sup> mice.** **A**, General overview showing generation of the *CNS28*<sup>-/-</sup> mouse using recombinase mediated cassette exchange (RMCE). Briefly, the region of the wild-type (WT) mouse *Scn5a* locus between sites (1) and (3), including exon 2 and portions of introns 1 and 2, was previously modified by gene targeting to contain 2 inversely oriented LoxP sites flanking a cassette that contains a neomycin resistant gene and the thymidine kinase (TK) gene.<sup>19</sup> An exchange vector that includes the human *SCN5A* cDNA flanked by the portions of introns 1 and 2 in the targeted regions was previously used to generate H/H mice. In the present experiment, the exchange vector was modified to remove a 435-bp fragment in intron 1 to generate the *CNS28*<sup>-/-</sup> mice. The 5' end of *CNS28* is located 1361 bp upstream from the

start of exon 2. A hygromycin-resistance cassette in the exchanged DNA was removed by breeding to FlpE-expressing animals, leaving a single residual FRT site. **B**, Genotyping reaction across *CNS28* showing H/H, *CNS28*<sup>+/-</sup>, and *CNS28*<sup>-/-</sup>. These lanes were run on the same gel but were noncontiguous.

conservation across species at the SRF and at one of the TEF-1 sites. Accordingly, our further studies focused on the activity of *CNS28*, a 435-bp region located in the 5' portion of intron 1.

**Generating *CNS28*<sup>-/-</sup> Mice**

In our previous studies, we replaced a region flanking the endogenous exon 2 transcription site with a construct that contained approximately 2 kb of mouse intron 1 along with

the human *SCN5A* cDNA. In homozygous mice, designated H/H, no murine *Scn5a* expression was detected; ventricular myocyte sodium current and electrocardiograms (ECGs) were identical to those in wild-type animals, indicating that the human channel generated physiological channel function.<sup>19</sup> In the present experiments, we used site-directed mutagenesis to remove the *CNS28* element from our original exchange construct (Figure 2A) and then used RMCE to generate *CNS28*<sup>+/-</sup> mice. Loss of *CNS28* was confirmed by

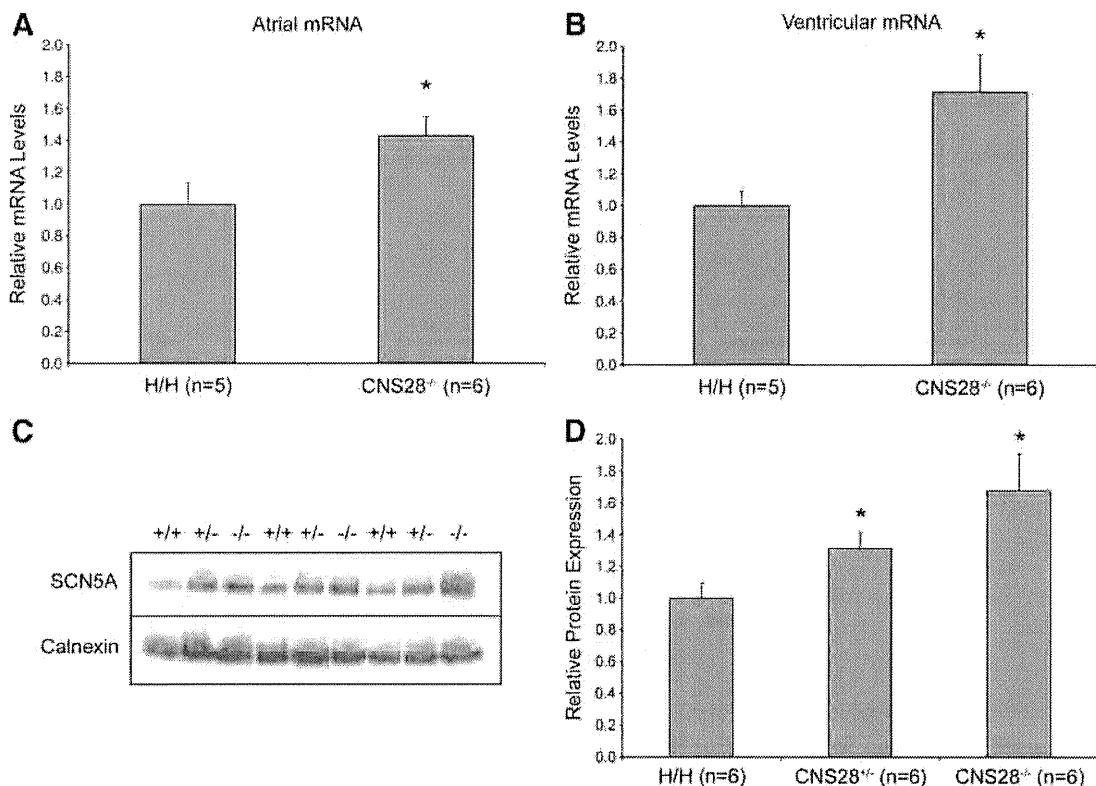


**Figure 3. Relative transcript and protein amounts in H/H and *CNS28*<sup>-/-</sup>.** *SCN5A* atrial mRNA (**A**) and ventricular mRNA (**B**) levels analyzed by quantitative real-time PCR. *CNS28*<sup>-/-</sup> mice had 42%±12% more expression in atria and 71%±23% more in ventricles than did H/H. **C**, Whole-heart protein expression levels analyzed by Western blot. Bands were analyzed on the same gel. **D**, Band densitometry analysis of the Western blots showing relative Na<sub>v</sub>1.5 amounts normalized to Calnexin. Na<sub>v</sub>1.5 abundance in heart was 31%±10% higher in *CNS28*<sup>+/-</sup> mice and 67%±23% higher in *CNS28*<sup>-/-</sup> mice. \*P<0.05 in comparison with H/H.

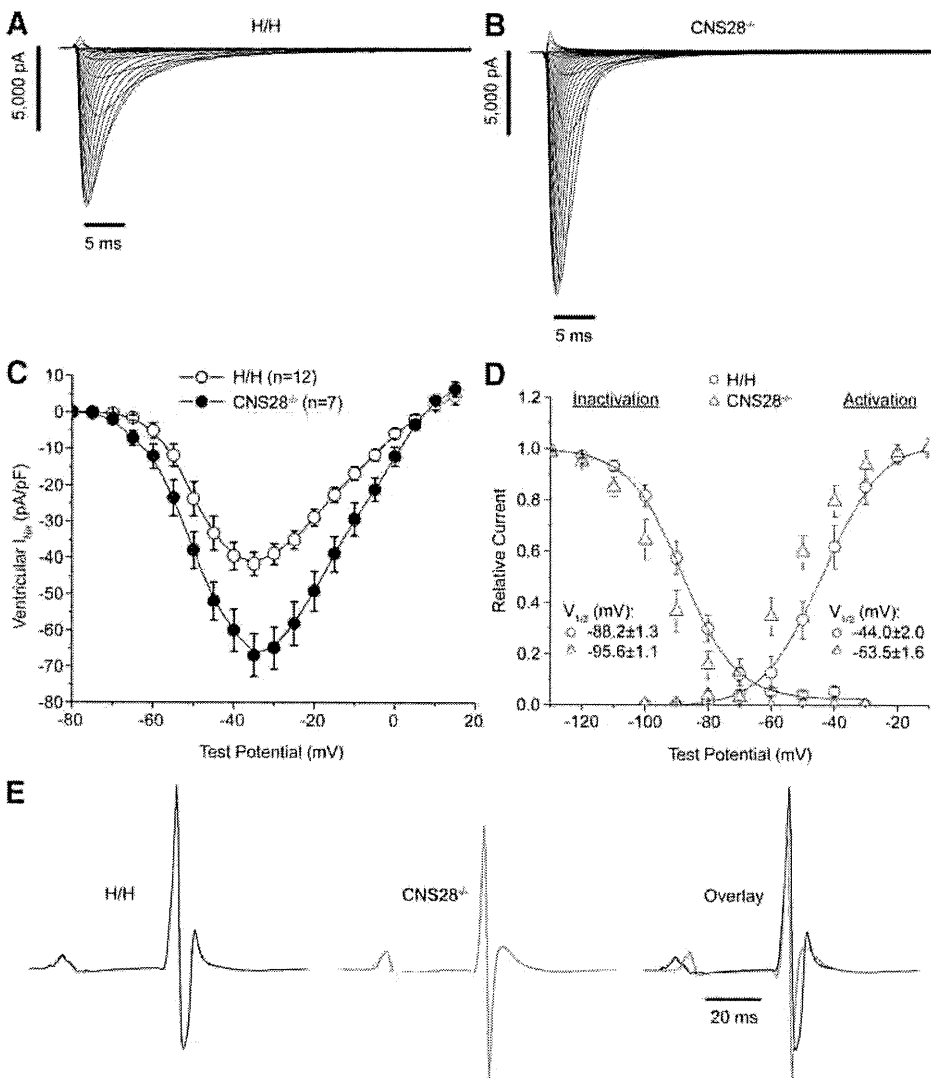


**Figure 4. Increased amounts of  $\text{Na}_v1.5$  in  $\text{CNS28}^{-/-}$  are functional.** Representative traces of  $\text{I}_{\text{Na}}$  from a ventricular myocyte isolated from either an H/H (A) or  $\text{CNS28}^{-/-}$  (B) mouse. C, Current-voltage relationship was evaluated in H/H and  $\text{CNS28}^{-/-}$  mice.  $\text{I}_{\text{Na}}$  amplitude measured at  $-30$  mV was  $59\% \pm 14\%$  greater in  $\text{CNS28}^{-/-}$  ventricular myocytes than in H/H cells. D, Voltage dependence of activation and inactivation measured in isolated ventricular myocytes in which we observed small but significant negative shifts in the voltage dependence of sodium channel activation and inactivation in  $\text{CNS28}^{-/-}$ . E, Representative ECG traces averaged over 10-second intervals for H/H and  $\text{CNS28}^{-/-}$  mice.  $\text{CNS28}^{-/-}$  mice display 12.3% shorter PR intervals, 9.3% shorter QRS intervals, and 7.0% shorter QT intervals than do H/H.  $P < 0.05$  in comparison with H/H.

genotyping (Figure 2B), and matings of  $\text{CNS28}^{+/-} \times \text{CNS28}^{+/-}$  mice yielded pup distributions in Hardy Weinberg equilibrium with 32 H/H, 64  $\text{CNS28}^{+/-}$ , and 41  $\text{CNS28}^{-/-}$ .

### Sodium Channel Expression in $\text{CNS28}^{-/-}$ Mice

Our initial results indicated that the  $\text{CNS28}$  fragment increased SV40-mediated reporter activity. However, in  $\text{CNS28}^{-/-}$  mouse hearts, quantitative real-time PCR (qPCR) showed that *SCN5A* transcripts levels were  $42\% \pm 12\%$  more abundant in atria and  $71\% \pm 23\%$  more abundant in ventricles than in H/H mice ( $P < 0.05$  in both tissues, Figure 3A and 3B). Western blotting showed concordant results: calnexin-normalized  $\text{Na}_v1.5$  abundance in heart was  $31\% \pm 10\%$  higher in  $\text{CNS28}^{+/-}$  and  $67\% \pm 23\%$  higher in  $\text{CNS28}^{-/-}$  mice than in H/H mice ( $P < 0.05$  for both  $\text{CNS28}^{+/-}$  and  $\text{CNS28}^{-/-}$  when compared with H/H, Figure 3C and 3D).

These changes translated into increases in functional sodium channels (Figure 4A and 4B). Peak  $\text{I}_{\text{Na}}$  amplitude measured at  $-30$  mV was  $59\% \pm 14\%$  greater in  $\text{CNS28}^{-/-}$  ventricular myocytes in comparison with that in H/H cells ( $P < 0.05$ , Figure 4C). Interestingly, we also observed small but significant negative shifts in the voltage dependence of

sodium channel activation and inactivation in  $\text{CNS28}^{-/-}$  myocytes (Figure 4D).

$\text{CNS28}^{-/-}$  mice also showed ECG changes consistent with these findings. In comparison with WT, homozygotes displayed 12.3% shorter PR intervals ( $38.8 \pm 0.6$  ms versus  $34.1 \pm 0.7$  ms), 9.3% shorter QRS intervals ( $10.7 \pm 0.2$  ms versus  $9.7 \pm 0.2$  ms), and 7.0% shorter QT intervals ( $52.9 \pm 0.8$  ms versus  $49.2 \pm 1.2$  ms) (all  $P < 0.05$ , Figure 4E). After challenge with the sodium channel blocker lidocaine, these intervals increased to a similar absolute extent in both genotypes, prolonging PR by 14.1 and 13.9 ms and QRS by 4.1 and 3.2 ms in H/H and  $\text{CNS28}^{-/-}$ , respectively. Flecainide challenge showed similar results (data not shown).

### In Vitro Transcriptional Regulation by $\text{CNS28}$

The finding that deleting  $\text{CNS28}$  increased channel transcripts and protein, with functional consequences, indicates that this region includes sequences that suppress sodium channel expression in vivo. This result is at odds with the initial screening experiment that identified  $\text{CNS28}$  as a potential positive regulatory sequence.

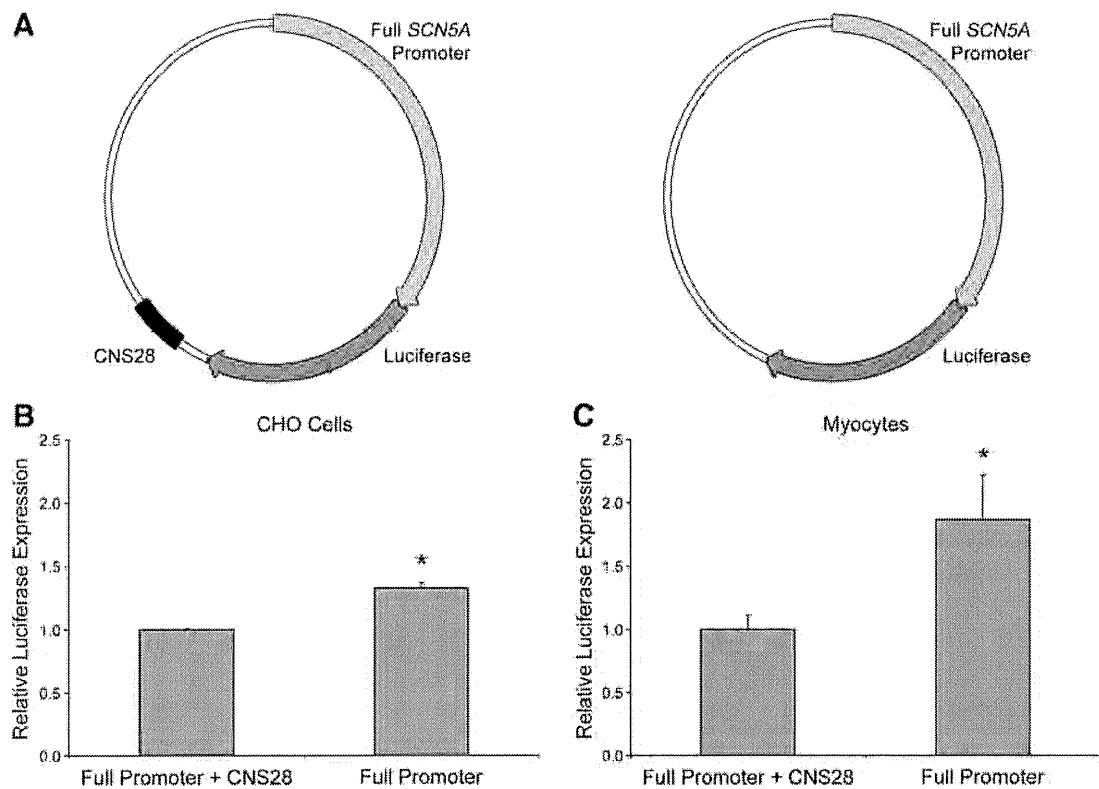


**Figure 5. Activity of human CNS28 on the full-length human *SCN5A* promoter.** **A**, Graphical representation of the vectors used. Luciferase activity driven by the full-length human *SCN5A* promoter with and without CNS28 in CHO cells (**B**) and neonatal cardiomyocytes (**C**). *SCN5A* promoter with CNS28 is designated 100% activity. When CNS28 is not present, luciferase activity increases by  $33\% \pm 4\%$  in CHO cells and  $87\% \pm 35\%$  in myocytes.  $*P < 0.05$ .

On the basis of these results we assessed reporter activity of constructs in which human CNS28 was included with the full-length *SCN5A* promoter<sup>6</sup> rather than the SV40 promoter used in the initial experiments. We compared activity of 2 constructs, each containing the *SCN5A* promoter and luciferase, 1 with and 1 without CNS28 (Figure 5A). The construct without CNS28 increased luciferase expression  $33\% \pm 4\%$  in CHO cells and  $87\% \pm 35\%$  in myocytes (Figure 5B and 5C, both  $P < 0.05$ ), consistent with the repressor function indicated by the in vivo findings.

We have previously identified a region upstream of exon 1 as the core *SCN5A* promoter.<sup>5,6</sup> Experiments conducted by Shang and Dudley revealed a second, 1363-bp *Scn5a* promoter in the mouse.<sup>9</sup> The 5' 435 bp of this promoter are what we identified in our screen as CNS28. Their analysis suggested that the 5' 480 bp contained a repressive element.<sup>9</sup> We hypothesized that CNS28 contained this repressive activity and generated a series of smaller deletions of the alternative promoter that they described (Figure 6A). The rVista analysis identified 30 possible transcription factor-binding sites conserved between the human and mouse, and therefore break points were chosen between clusters of these sites (Online Figure 1). The full alternative promoter-luciferase construct (1,361 bp) was designated deletion construct 0 (DC0), and contains all the features of the Shang and Dudley promoter stated above. Deletion construct 1 (DC1) removes the initial 50 bp and deletion construct 2 (DC2) an additional 100 bp. Deletion construct 3 (DC3) eliminates 285 bp of the alternate promoter.

Deletion construct 4 (DC4) takes away the entirety of CNS28 from the alternate promoter by deleting the first 435 bp.

In our luciferase reporter assay, the activity of DC0 was used as the baseline reference in both CHO cells and myocytes. Constructs DC1 and DC2 showed no difference in activity versus DC0 in either cell type. The DC3 construct virtually abolished reporter activity in both cell types, reducing activity to  $3.3\% \pm 0.1\%$  of DC0 in CHO cells, and  $12\% \pm 3\%$  in myocytes (both  $P < 0.05$ ). The last construct, DC4, restored activity to  $79\% \pm 6\%$  and  $67\% \pm 11\%$  of DC0 in CHO cells and myocytes, respectively (Figure 6B and 6C, both  $P < 0.05$ ). There are 2 points illustrated by these data. First, between DC2 and DC3 there is likely an enhancer element that can counter the negative transcriptional activity we observe with CNS28; therefore, DC3 shows the highest repressive activity. Second, removal of 150 base pairs between DC3 and DC4 results in loss of that repressive activity. Sequence analysis of this region shows that it contains an E-box motif (consensus sequence CANNTG).<sup>23</sup> The repressor Snail has previously been shown to bind E-boxes in the core promoter of *SCN5A*.<sup>7</sup> Therefore we tested the hypothesis that this E-box may be important for repressor binding. When the motif was mutated in DC3 (CATATG to CTTAAG), activity was restored to  $62\% \pm 4\%$  of the activity of DC0 in CHO cells and  $66\% \pm 10\%$  in myocytes (Figure 6D and 6E, both  $P < 0.05$ ). This increase in activity is similar to the increase we see between DC3 and DC4, in which the final segment containing the E-box is removed, further supporting our hypothesis.



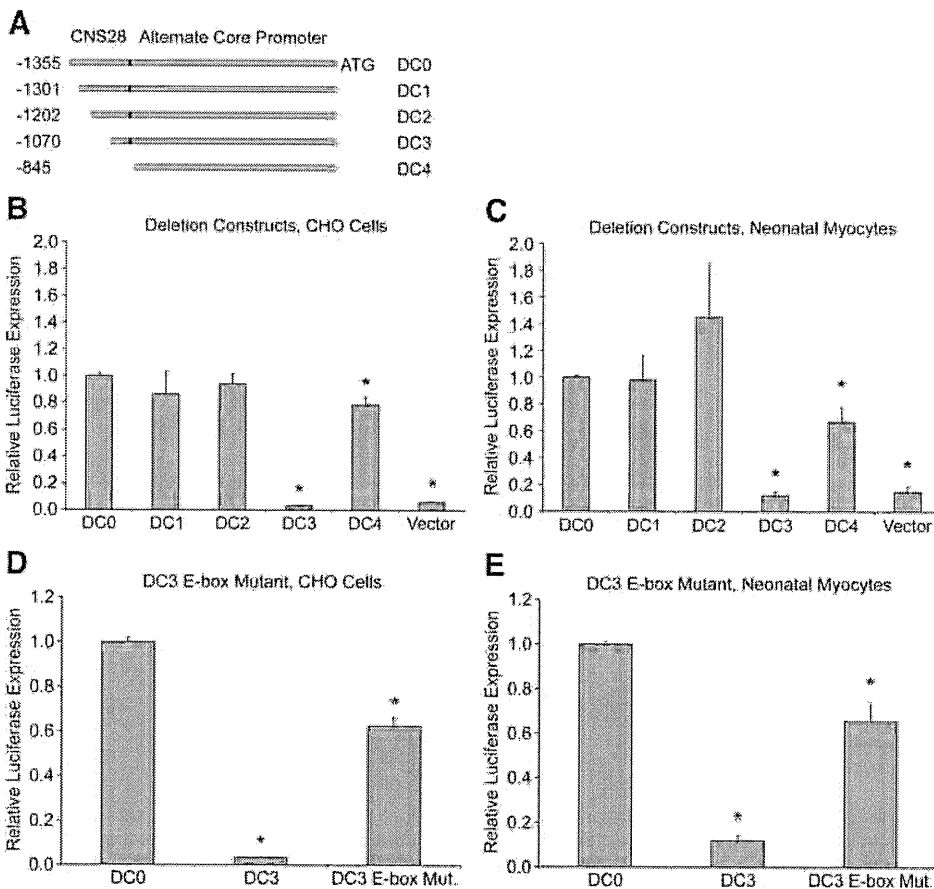


**Figure 6. Progressive deletion construct analysis of the alternate promoter.** **A**, A schematic showing the progressive truncations of the CNS28 portion of the mouse alternate promoter in the luciferase constructs used. The translation start site is designated as +1. Analysis of the deletion constructs in CHO cells (**B**) or neonatal myocytes (**C**). DC0 is designated 100% activity. DC3, which deletes the majority of CNS28 from DC0, reduced reporter activity in both cell types to  $3.3\pm 0.1\%$  of DC0 in CHO cells, and  $12\pm 3\%$  in myocytes. Removal of the last portion of CNS28, DC4, restored activity close to baseline. Mutating the E-box consensus sequence in DC3 restores reporter activity to  $62\pm 4\%$  of the activity of DC0 in CHO cells (**D**) and  $66\pm 10\%$  in myocytes (**E**). \* $P < 0.05$  in comparison with DC0.

## Discussion

### Sodium Channels Are Required for Normal Cardiac Function

$\text{Na}_v1.5$  expression is absolutely required for normal cardiac function; knockouts in mice and in fish are embryolethal and cause cardiac developmental abnormalities.<sup>24,25</sup> More modest reduction of sodium current slows cardiac conduction and creates an arrhythmia-prone heart in the setting of monogenic disease<sup>26,27</sup> or during therapy with sodium channel-blocking drugs.<sup>4</sup> We have previously found an association between a variant haplotype in a regulatory region of the cardiac sodium channel promoter commonly observed in Asian subjects and variable QRS duration, and recent genome-wide association studies have identified an association between the *SCN5A-10A* locus and variable PR and QRS durations.<sup>28–30</sup> These data support the general hypothesis<sup>31,32</sup> that variable cardiac ion channel transcription modulates the electrophysiological properties of the heart. A contrary view is that feedback mechanisms in the mammalian heart regulate transcription to achieve a tight range of normal electrophysiological behaviors,<sup>32</sup> although monogenic diseases producing striking electrocardiographic changes argue against such tight control. Previous work in this area has focused on in vitro approaches and on establishing the functional consequences of coding region variants in genetically modified mice. However, no study to date has directly evaluated the functional consequences of deleting noncoding potential regulatory regions of a cardiac ion channel gene.

### CNS28 Regulates Cardiac Sodium Channel Expression

Our initial in silico screen identified 92 highly conserved noncoding sequences, and preliminary reporter experiments, using the SV40 promoter, suggested that one, CNS28, included positive regulatory elements for *SCN5A*. Driven by this initial result, we generated *CNS28*<sup>-/-</sup> mice, and unexpectedly, these animals demonstrated dramatic increases in sodium channel transcripts and channel protein expression. This increased  $\text{Na}_v1.5$  is functional: the *CNS28*<sup>-/-</sup> mice have significantly larger peak  $I_{\text{Na}}$  in isolated ventricular myocytes and shorter PR and QRS, indicating rapid ventricular conduction. The increased sodium current also displayed unexpected shifts in the voltage dependence of channel activation and inactivation; the mechanism requires further study, but one possibility is a change in the extent of interaction with ancillary proteins, such as  $\beta$ -subunits, that are known to modulate channel gating.<sup>33</sup> For example, using real-time PCR, we found no alterations in expression of *Scn1b* in *CNS28*<sup>-/-</sup> mouse hearts (Online Figure II). This supports the notion that although more sodium channels are present, concomitant increases in function modifying protein partners may not occur. Changes in the  $\text{Na}_v1.5$  macromolecular complex could lead to alteration in channel gating. Further experiments examining changes in expression and localization of other  $\text{Na}_v1.5$  partners<sup>34</sup> may assist in elucidating the underlying mechanism. Another possibility is raised by the clustering of *Scn5a* with *Scn10a* and *11a* in the mouse and

human genomes; thus, it is conceivable that removal of CNS28 impacts the level of expression of these channels in the heart. Such a change in the channel profile in the heart could result in shifts in the inactivation and activation of cardiac sodium current. However, in preliminary experiments we observe no change in *Scn11a* expression in the 2 lines and have been unable to amplify *Scn10a*, suggesting that this channel is not abundantly expressed in the heart. Importantly, heart wall measurements, examination of contractile function (Online Table II), and survival rates were no different in CNS28<sup>-/-</sup> mice than they were in H/H animals.

### Molecular Basis for CNS28 Activity

Our study identified a 435-bp segment of DNA whose deletion increases channel expression, and reporter experiments using the more physiologically relevant *SCN5A* promoter are consistent with this result. Our analysis of deletion constructs demonstrates that a repressor element lies within a 226-bp fragment at the 3' end of CNS28. The 5 binding sites conserved between mouse and human in this region identified by rVista include E47, E12, E2A, MYOD, and T3R. None of these factors are good candidates to act as a repressor. However, in the 226-bp segment, we also identified a single E-box motif in the mouse and 2 in the human. Mice overexpressing Snail, which binds E-box sites in the *SCN5A* core promoter, exhibit a reduction in *Scn5A* transcript and protein.<sup>7</sup> We observed an increase in luciferase expression following mutation of the E-box, arguing that this motif is critical for repression of *SCN5A*. E-boxes are typically bound by basic helix-loop-helix factors, such as HAND proteins.<sup>23</sup> However, given the previous studies linking Snail to *SCN5A*, our work raises the possibility that the CNS28 E-box is a Snail-binding region and that this interaction is needed in vivo to regulate *SCN5A* transcript levels.

### Limitations

One limitation of our study is that in order to identify elements relevant to *SCN5A* transcription, we choose to examine highly conserved elements between the mouse and human and replace the mouse *Scn5a* allele with a human *SCN5A*. However, in the animals we generated, potential mouse regulatory sequences, including the core promoter, are intact, and therefore the effects we see following deletion of CNS28 are in the murine context and may or may not apply to humans. However, E-boxes are evolutionarily conserved in both mouse and human promoter regions and so likely have similar functions in both species.

### Summary

We hypothesize that increased sodium channel expression should translate to protection against arrhythmias that are mediated by decreased sodium channel function; settings in which this mechanism is thought to be operative include acute ischemia, especially with sodium channel block<sup>4</sup> and the Brugada Syndrome.<sup>3,25,35</sup> As a first test of this hypothesis, we examined the extent to which challenge with a sodium channel blocker slowed conduction in H/H and CNS28<sup>-/-</sup> mice. In this experiment, both lidocaine and flecainide prolonged PR and QRS to a similar extent; thus, with drug challenge, absolute conduction

times remained shorter in the CNS28<sup>-/-</sup> animals. The further elucidation of mechanisms affecting *SCN5A* transcription may point to entirely novel ways in which to intervene to stabilize cardiac electrophysiological activity.

### Acknowledgments

We would like to acknowledge Wei Zhang for animal care and technical assistance.

### Sources of Funding

This work was supported by grants from the United States Public Health Service (HL49989, HL65962).

### Disclosures

The authors have no conflicts of interest to declare.

### References

- George AL. Inherited disorders of voltage-gated sodium channels. *J Clin Invest*. 2005;115:1990–1999.
- Balser JR. Inherited sodium channelopathies. Novel therapeutic and proarrhythmic molecular mechanisms. *Trends Cardiovasc Med*. 2001;11:229–237.
- Bezzina CR, Shimizu W, Yang P, Koopmann TT, Tanck MWT, Miyamoto Y, Kamakura S, Roden DM, Wilde AAM. Common sodium channel promoter haplotype in Asian subjects underlies variability in cardiac conduction. *Circulation*. 2006;113:338–344.
- Cardiac Arrhythmia Suppression Trial (CAST) investigators. Preliminary report: effect of encainide and flecainide on mortality in a randomized trial of arrhythmia suppression after myocardial infarction. The Cardiac Arrhythmia Suppression Trial (CAST) investigators. *N Engl J Med*. 1989;321:406–412.
- Yang P, Koopmann TT, Pfeufer A, Jalilzadeh S, Schulze-Bahr E, Kaab S, Wilde AA, Roden DM, Bezzina CR. Polymorphisms in the cardiac sodium channel promoter displaying variant in vitro expression activity. *Eur J Hum Genet*. 2007;16:350–357.
- Yang P, Kupersmidt S, Roden DM. Cloning and initial characterization of the human cardiac sodium channel (SCN5A) promoter. *Cardiovasc Res*. 2004;61:56–65.
- Hesse M, Kondo CS, Clark RB, Su L, Allen FL, Geary-Joo CTM, Kunnathu S, Severson DL, Nygren A, Giles WR, Cross JC. Dilated cardiomyopathy is associated with reduced expression of the cardiac sodium channel *Scn5a*. *Cardiovasc Res*. 2007;75:498–509.
- Nieto MA. The snail superfamily of zinc-finger transcription factors. *Nat Rev Mol Cell Biol*. 2002;3:155–166.
- Shang LL, Dudley SC. Tandem promoters and developmentally regulated 5' and 3' mRNA untranslated regions of the mouse *Scn5a* cardiac sodium channel. *J Biol Chem*. 2005;280:933–940.
- Dubchak I, Brudno M, Loots GG, Pachter L, Mayor C, Rubin EM, Frazer KA. Active conservation of noncoding sequences revealed by three-way species comparisons. *Genome Res*. 2000;10:1304–1306.
- Mayor C, Brudno M, Schwartz JR, Poliakov A, Rubin EM, Frazer KA, Pachter LS, Dubchak I. VISTA. Visualizing global DNA sequence alignments of arbitrary length. *Bioinformatics*. 2000;16:1046–1047.
- Alkema WBL, Johansson O, Lagergren J, Wasserman WW. MSCAN. Identification of functional clusters of transcription factor binding sites. *Nucl Acids Res*. 2004;32:W195–W198.
- Johansson O, Alkema W, Wasserman WW, Lagergren J. Identification of functional clusters of transcription factor binding motifs in genome sequences: the MSCAN algorithm. *Bioinformatics*. 2003;19:i169–i176.
- Loots GG, Ovcharenko I. rVISTA 2.0: evolutionary analysis of transcription factor binding sites. *Nucl Acids Res*. 2004;32:W217–W221.
- Ovcharenko I, Loots GG, Hardison RC, Miller W, Stubbs L. zPicture: dynamic alignment and visualization tool for analyzing conservation profiles. *Genome Res*. 2004;14:472–477.
- Lowe JS, Palygin O, Bhasin N, Hund TJ, Boyden PA, Shibata E, Anderson ME, Mohler PJ. Voltage-gated Nav channel targeting in the heart requires an ankyrin-G dependent cellular pathway. *J Cell Biol*. 2008;180:173–186.
- Jones, JR, Shelton, KD, Magnuson, MA. Strategies for the use of site-specific recombinases in genome engineering. *Methods Mol Med*. 2005; 103:245–257.
- Seibler J, Schubeler D, Fiering S, Groudine M, Bode J. DNA cassette exchange in ES cells mediated by FLP recombinase: an efficient strategy

- for repeated modification of tagged loci by marker-free constructs. *Biochemistry*. 1998;37:6229–6234.
19. Liu K, Hipkens S, Yang T, Abraham R, Zhang W, Chopra N, Knollmann B, Magnuson MA, Roden DM. Recombinase-mediated cassette exchange to rapidly and efficiently generate mice with human cardiac sodium channels. *Genesis*. 2006;44:556–564.
  20. Knollmann BC, Chopra N, Hlaing T, Akin B, Yang T, Etensohn K, Knollmann BEC, Horton KD, Weissman NJ, Holinstat I, Zhang W, Roden DM, Jones LR, Franzini-Armstrong C, Pfeiffer K. Casq2 deletion causes sarcoplasmic reticulum volume increase, premature Ca<sup>2+</sup> release, and catecholaminergic polymorphic ventricular tachycardia. *J Clin Invest*. 2006;116:2510–2520.
  21. Mitra R, Morad M. A uniform enzymatic method for dissociation of myocytes from hearts and stomachs of vertebrates. *Am J Physiol*. 1985;249:H1056–H1060.
  22. Rottman JN, Ni G, Brown M. Echocardiographic evaluation of ventricular function in mice. *Echocardiography*. 2007;24:83–89.
  23. Massari ME, Murre C. Helix-loop-helix proteins: regulators of transcription in eucaryotic organisms. *Mol Cell Biol*. 2000;20:429–440.
  24. Chopra SS, Stroud DM, Watanabe H, Bennett JS, Burns CG, Wells KS, Yang T, Zhong TP, Roden DM. Voltage-gated sodium channels are required for heart development in zebrafish. *Circ Res*. 2010;106:1342–1350.
  25. Papadatos GA, Wallerstein PMR, Head CEG, Ratcliff R, Brady PA, Benndorf K, Saumarez RC, Trezise AEO, Huang CLH, Vandenberg JJ, Colledge WH, Grace AA. Slowed conduction and ventricular tachycardia after targeted disruption of the cardiac sodium channel gene *Scn5a*. *Proc Natl Acad Sci U S A*. 2002;99:6210–6215.
  26. Antzelevitch C, Brugada P, Borggreffe M, Brugada J, Brugada R, Corrado D, Gussak I, LeMarec H, Nademanee K, Perez Riera AR, Shimizu W, Schulze-Bahr E, Tan H, Wilde A. Brugada syndrome: report of the Second Consensus Conference: endorsed by the Heart Rhythm Society and the European Heart Rhythm Association. *Circulation*. 2005;111:659–670.
  27. Kapplinger JD, Tester DJ, Alders M, Benito Ba, Berthet M, Brugada J, Brugada P, Fressart V, Guerchicoff A, Harris-Kerr C, Kamakura S, Kyndt F, Koopmann TT, Miyamoto Y, Pfeiffer R, Pollevick GD, Probst V, Zumhagen S, Vatta M, Towbin JA, Shimizu W, Schulze-Bahr E, Antzelevitch C, Salisbury BA, Guicheney P, Wilde AAM, Brugada R, Schott JJ, Ackerman MJ. An international compendium of mutations in the *SCN5A*-encoded cardiac sodium channel in patients referred for Brugada syndrome genetic testing. *Heart Rhythm*. 2010;7:33–46.
  28. Chambers JC, Zhao J, Terracciano CMN, Bezzina CR, Zhang W, Kaba R, Navaratnarajah M, Lotlikar A, Sehmi JS, Kooner MK, Deng G, Siedlecka U, Parasramka S, El-Hamamsy I, Wass MN, Dekker LRC, de Jong JSSG, Sternberg MJE, McKenna W, Severs NJ, de Silva R, Wilde AAM, Anand P, Yacoub M, Scott J, Elliott P, Wood JN, Kooner JS. Genetic variation in *SCN10A* influences cardiac conduction. *Nat Genet*. 2010;42:149–152.
  29. Holm H, Gudbjartsson DF, Arnar DO, Thorleifsson G, Thorgeirsson G, Stefansdottir H, Gudjonsson SA, Jonasdottir A, Mathiesen EB, Njolstad I, Nyrnes A, Wilsgaard T, Hald EM, Hveem K, Stoltenberg C, Lochen ML, Kong A, Thorsteinsdottir U, Stefansson K. Several common variants modulate heart rate, PR interval and QRS duration. *Nat Genet*. 2010;42:117–122.
  30. Pfeufer A, van Noord C, Marcianti KD, Arking DE, Larson MG, Smith AV, Tarasov KV, Muller M, Sotoodehnia N, Sinner MF, Verwoert GC, Li M, Kao WHL, Kottgen A, Coresh J, Bis JC, Psaty BM, Rice K, Rotter JI, Rivadeneira F, Hofman A, Kors JA, Stricker BHC, Uitterlinden AG, van Duijn CM, Beckmann BM, Sauter W, Gieger C, Lubitz SA, Newton-Cheh C, Wang TJ, Magnani JW, Schnabel RB, Chung MK, Barnard J, Smith JD, Van Wagener DR, Vasan RS, Aspelund T, Eiriksdottir G, Harris TB, Launer LJ, Najjar SS, Lakatta E, Schlessinger D, Uda M, Abecasis GR, Muller-Myhsok B, Ehret GB, Boerwinkle E, Chakravarti A, Soliman EZ, Lunetta KL, Perz S, Wichmann HE, Meitinger T, Levy D, Gudnason V, Ellinor PT, Sanna S, Kaab S, Witteman JCM, Alonso A, Benjamin EJ, Heckbert SR. Genome-wide association study of PR interval. *Nat Genet*. 2010;42:153–159.
  31. Arking DE, Chugh SS, Chakravarti A, Spooner PM. Genomics in sudden cardiac death. *Circ Res*. 2004;94:712–723.
  32. Rosati B, McKinnon D. Regulation of ion channel expression. *Circ Res*. 2004;94:874–883.
  33. Aman TK, Grieco-Calub TM, Chen C, Rusconi R, Slat EA, Isom LL, Raman IM. Regulation of persistent Na current by interactions between {beta} subunits of voltage-gated Na channels. *J Neurosci*. 2009;29:2027–2042.
  34. Abriel H. Cardiac sodium channel Nav1.5 and interacting proteins: physiology and pathophysiology. *J Mol Cell Cardiol*. 2010;48:2–11.
  35. Ruan Y, Liu N, Priori SG. Sodium channel mutations and arrhythmias. *Nat Rev Cardiol*. 2009;6:337–348.

## Novelty and Significance

### What Is Known?

- Decreased cardiac sodium current, through mutations or drug block, increases susceptibility to brady- and tachyarrhythmias.
- Although in vitro experiments have identified putative regulatory elements in the cardiac sodium channel genes *SCN5A*, the extent to which these alter channel function in vivo is unknown.

### What New Information Does This Article Contribute?

- We identify multiple noncoding regions in *SCN5A* displaying cross-species sequence conservation.
- Informatic and promoter-reporter studies implicate one of these, conserved noncoding sequence 28 (CNS28), as a potential regulator of channel expression.
- We have compared *SCN5A* expression and function in mice with humanized cardiac sodium channels to mice that are identical, except that they lack a 435-bp fragment, which includes CNS28, in intron 1.
- Removal of these 435 bp increases *SCN5A* expression and sodium current amplitude, and speeds cardiac conduction.
- Deletion of a putative Snail binding region within the 435-bp element partially relieves its repressive activity.

Multiple lines of evidence suggest that reduced expression of the human cardiac sodium channel gene *SCN5A* can lead to arrhythmias. However, no study to date has explored the in vivo consequences of deleting potential regulatory noncoding regions of a cardiac ion gene. In this study we first identified conserved noncoding sequences (CNS) when the mouse and human genes were compared. Initial experiments identified one, CNS28, as a potential regulator of channel expression. We have previously generated mice in which the murine ortholog *Scn5a* is ablated and the human *SCN5A* cDNA expressed in its place. In the present experiments, we generated mice in which a 435-bp region encompassing CNS28 was removed. Removing CNS28 increased *SCN5A* mRNA, protein, and sodium current, and was associated with enhanced conduction (decreased PR and QRS intervals). Promoter-reporter experiments showed that removal of an E-box in CNS28 increased reporter activity. These findings support the hypothesis that variable expression of cardiac ion channels can alter the electrophysiological properties of the intact heart. Understanding the mechanisms underlying ion channel regulation could lead to potential new therapies for arrhythmias.

This Review is the last in a thematic series on **Inherited Arrhythmogenic Syndromes: The Molecular Revolution**, which includes the following articles:

The Fifteen Years that Shaped Molecular Electrophysiology: Time for Appraisal [*Circ Res.* 2010;107:451–456]

Defining a New Paradigm for Human Arrhythmia Syndromes: Phenotypic Manifestations of Gene Mutations in Ion Channel- and Transporter-Associated Proteins [*Circ Res.* 2010;107:457–465]

The Cardiac Desmosome and Arrhythmogenic Cardiomyopathies: From Gene to Disease [*Circ Res.* 2010;107:700–714]

Phenotypical Manifestations of Mutations in the Genes Encoding Subunits of the Cardiac voltage-dependent L-type Calcium Channel [*Circ Res.* 2011;108:607–618]

Inherited dysfunction of Sarcoplasmic Reticulum Ca<sup>2+</sup> Handling and Arrhythmogenesis [*Circ Res.* 2011;108:871–883]

Phenotypical Manifestations of Mutations in the Genes Encoding Subunits of the Cardiac Sodium Channel [*Circ Res.* 2011;108:884–897]

Phenotypical Manifestations of Mutations in Genes Encoding Subunits of Cardiac Potassium Channels

*Silvia Priori, Editor*

## Phenotypic Manifestations of Mutations in Genes Encoding Subunits of Cardiac Potassium Channels

Wataru Shimizu, Minoru Horie

**Abstract:** Since 1995, when a potassium channel gene, *hERG* (human ether-à-go-go-related gene), now referred to as *KCNH2*, encoding the rapid component of cardiac delayed rectifier potassium channels was identified as being responsible for type 2 congenital long-QT syndrome, a number of potassium channel genes have been shown to cause different types of inherited cardiac arrhythmia syndromes. These include congenital long-QT syndrome, short-QT syndrome, Brugada syndrome, early repolarization syndrome, and familial atrial fibrillation. Genotype-phenotype correlations have been investigated in some inherited arrhythmia syndromes, and as a result, gene-specific risk stratification and gene-specific therapy and management have become available, particularly for patients with congenital long-QT syndrome. In this review article, the molecular structure and function of potassium channels, the clinical phenotype due to potassium channel gene mutations, including genotype-phenotype correlations, and the diverse mechanisms underlying the potassium channel gene-related diseases will be discussed. (*Circ Res.* 2011;109:97-109.)

**Key Words:** genetic testing ■ ion channels ■ sudden death ■ ventricular fibrillation ■ atrial fibrillation

A variety of mutations in genes that encode cardiac potassium channel pore-forming proteins and their accessory modulating proteins have been shown to cause different types of inherited arrhythmias. Such results were made possible by either candidate gene or linkage studies. Candidate gene studies examine variations in a low number of

known, plausibly associated genes in affected case and control subjects, whereas linkage studies assess affected families/sibling pairs by use of microsatellite markers to define a genomic region linked to the phenotype. These approaches have resulted in an understanding of the genetic background of cardiac ion channelopathies, including

Original received February 15, 2011; revision received April 4, 2011; accepted April 19, 2011. In March 2011, the average time from submission to first decision for all original research papers submitted to *Circulation Research* was 13.2 days.

From the Division of Arrhythmia and Electrophysiology, Department of Cardiovascular Medicine, National Cerebral and Cardiovascular Center (W.S.), Suita, Japan, and the Department of Cardiovascular and Respiratory Medicine, Shiga University of Medical Science (M.H.), Otsu, Japan.

Drs Shimizu and Horie contributed equally to this review article.

Correspondence to Dr Wataru Shimizu, Division of Arrhythmia and Electrophysiology, Department of Cardiovascular Medicine, National Cerebral and Cardiovascular Center, 5-7-1 Fujishiro-dai, Suita, Osaka, 565-8565 Japan (E-mail wshimizu@hsp.ncvc.go.jp); or Dr Minoru Horie, Department of Cardiovascular and Respiratory Medicine, Shiga University of Medical Science, Otsu, Shiga 520-2192, Japan (E-mail Horie@belle.shiga-med.ac.jp).

© 2011 American Heart Association, Inc.

*Circulation Research* is available at <http://circres.ahajournals.org>

DOI: 10.1161/CIRCRESAHA.110.224600

Non-standard Abbreviations and Acronyms	
APD	action potential duration
BrS	Brugada syndrome
SQTS	short-QT syndrome

long-QT syndrome (LQTS).<sup>1</sup> In 1991, Keating and coworkers<sup>2</sup> used linkage analyses and first reported that a DNA marker at the Harvey ras-1 locus (H-ras-1) in chromosome 11 was linked to LQTS. Five years later, in 1996, positional cloning methods established a potassium channel gene, *KVLQT1*, now referred to as *KCNQ1*, as the chromosome 11-linked LQT1 gene.<sup>3</sup> One year earlier, in 1995, another potassium channel gene, *hERG* (human ether-à-go-go-related gene), now referred to as *KCNH2*, was identified as being responsible for LQT2.<sup>4</sup> Since the mid-1990s, several potassium channel-encoding genes have been reported to be linked not only to LQTS but also to various inherited arrhythmia syndromes, including the short-QT syndrome (SQTS), Brugada syndrome (BrS), early repolarization syndrome, and familial atrial fibrillation (AF). Other potassium channel-encoding genes linked to various inherited arrhythmia syndromes include *KCNJ2*, *KCNJ5*, *KCNJ8*, and *KCNA5*, as well as the accessory subunits *KCNE1*, *KCNE2*, *KCNE3*, and *KCNE5* (Table).

### Molecular Structure and Function of Potassium Channels That Contribute to Formation of Cardiac Action Potential

An extensive diversity of potassium channels has been revealed since the first cloning of a voltage-gated potassium channel by Jan and colleagues.<sup>5</sup> This reflects the complex and multiple roles of potassium channels as modulators of physiological function. In the generation of cardiac action potential, for example, potassium channels work to maintain a hyperpolarized resting potential and determine the timing of repolarization by flowing outward currents during the plateau phase. Subtle and delicate expression of distinct types of potassium channels elegantly generates the whole-heart action potential gradient in both the transmural and apicobasal directions. Failure of their normal function may lead to various types of inherited arrhythmia syndromes, and in this regard, congenital LQTS has played the part of a Rosetta stone as predicted by Zipes 20 years ago.<sup>6</sup>

To generate the cardiac action potential, in addition to inward sodium and calcium currents, 5 potassium currents are primarily involved: The inward-rectifier background current ( $I_{K1}$ ), the rapidly activating and inactivating transient outward current ( $I_{to}$ ), and the ultrarapid ( $I_{Kur}$ ), rapid ( $I_{Kr}$ ), and slow ( $I_{Ks}$ ) components of delayed rectifier currents. (Abbreviations in parentheses indicate names of specific currents used in basic electrophysiology.)

$I_{K1}$  carries the background potassium current that stabilizes the resting membrane potential and is responsible for determining the threshold potential for the initial depolarization and final repolarization of the action potential (late phase 3).

**Table. Defect of Ion Channels or Membrane Adaptor Responsible for the Potassium Channel Gene-Related Arrhythmia Syndromes**

Loci	Chromosome	Gene	Ion Channel	Result
Congenital LQTS (Romano-Ward)				
LQT1	11 (11p15.5)	<i>KCNQ1</i>	$I_{Ks}$	Loss of function
LQT2	7 (7q35-q36)	<i>KCNH2</i>	$I_{Kr}$	Loss of function
LQT5	21 (21q22.12)	<i>KCNE1</i>	$I_{Ks}$	Loss of function
LQT6	21 (21q22.12)	<i>KCNE2</i>	$I_{Kr}$	Loss of function
LQT7	17 (17q23.1-q24.2)	<i>KCNJ2</i>	$I_{K1}$	Loss of function
LQT11	7 (7q21-q22)	<i>AKAP-9</i>	$I_{Ks}$	Loss of function
LQT13	11 (11q23.3-24.3)	<i>KCNJ5</i>	$I_{K-ACH}$	Loss of function
Congenital LQTS (Jervell and Lange-Nielsen)				
JLN1	11 (11p15.5)	<i>KCNQ1</i> (homozygous)	$I_{Ks}$	Loss of function
JLN2	21 (21q22.12)	<i>KCNE1</i> (homozygous)	$I_{Ks}$	Loss of function
SQTS				
SQT1	7 (7q35-q36)	<i>KCNH2</i>	$I_{Kr}$	Gain of function
SQT2	11 (11p15.5)	<i>KCNQ1</i>	$I_{Ks}$	Gain of function
SQT3	17 (17q23.1-q24.2)	<i>KCNJ2</i>	$I_{K1}$	Gain of function
Brugada syndrome				
BrS6	11 (11q13-q14)	<i>KCNE3</i>	$I_{to}$	Gain of function
Early repolarization syndrome				
	12 (12p11.23)	<i>KCNJ8</i>	$I_{K-ATP}$	Gain of function
Atrial fibrillation				
	11 (11p15.5)	<i>KCNQ1</i>	$I_{Ks}$	Gain of function
	21 (21q22.12)	<i>KCNE2</i>	$I_{Ks}$	Gain of function
	11 (11q13-q14)	<i>KCNE3</i>	$I_{Ks}$	Gain of function
	17 (17q23.1-q24.2)	<i>KCNJ2</i>	$I_{K1}$	Gain of function
	12 (12p13)	<i>KCNA5</i>	$I_{Kur}$	Loss of function

LQTS indicates long-QT syndrome; SQTS, short-QT syndrome.

$I_{to}$  consists of at least 2 components carrying fast ( $I_{to,f}$ ) and slow ( $I_{to,s}$ ) transient outward currents. They are differentiated on the basis of the rate of inactivation and its recovery and are variably expressed in the myocardium and form the transmural gradient of repolarization timing. Finally, delayed rectifier currents ( $I_K$ ) play a key role in determining the duration of action potentials and comprise at least 3 components:  $I_{Kur}$ ,  $I_{Kr}$ , and  $I_{Ks}$ . They are easily distinguished from each other by their pharmacological or biophysical properties.  $I_{Kur}$  is expressed mainly in the atrium and not in the ventricle and therefore does not help determine QT interval.<sup>7</sup>  $I_{Kr}$  activates rapidly but is easily inactivated on stronger depolarization (showing a strong inward rectification).<sup>8</sup> In contrast,  $I_{Ks}$  activates very slowly on depolarization compared with other potassium currents, and therefore, its net repolarizing currents can accumulate, especially at higher heart rates (because of a shorter diastolic phase) and are greatest at phase 3 of the action potential.<sup>8</sup> These fundamental understandings were mainly achieved since the late 1970s by means of patch-clamp techniques in mammalian cardiomyocytes.<sup>9</sup>

An understanding of the molecular biology of potassium channels came later, after the memorable report by Papazian et al.<sup>5</sup> The pore-forming subunit of the voltage-gated channel ( $\alpha$ -subunit) has since been shown to contain at least 2 highly conserved components: the voltage-sensing part that surrounds the central pore, and the pore domain itself. Voltage-gated potassium channels involved in formation of cardiac action potential work as a tetramer of  $\alpha$ -subunits, each having 6 transmembrane-spanning segments (S1–S6), with S4 containing 6 positively charged amino acids.<sup>10</sup> The pore domain is composed of S5, the P-loop, and S6, which is the ion permeation pathway, and includes the ion selectivity filter.<sup>11</sup> The opening of the channel and its associated gating current is caused by membrane depolarization and outward movement of the positively charged S4 segment. In addition to S4, the neighboring S2 and S3 segments serve as channel voltage sensors. Mutations in these regions may cause cardiac ion channel diseases by altering channel gating and ion permeability.<sup>12</sup>

*KCNH2* encodes the  $\alpha$ -subunit of the  $I_{Kr}$  channel, and membrane depolarization induced by strong inward currents produces a sequence of conformation changes within the channel that allows permeation of potassium ions. The S6 segment has a conserved glycine, which can be involved in channel opening by causing a wide splaying of the inner helices. When they close, these 4 inner helices, by leaning toward the membrane and interlace near the cytoplasmic border, narrow the ion passage and prevent potassium ion permeation.<sup>13</sup>

*KCNQ1* encodes the  $\alpha$ -subunit of  $I_{Ks}$  channels and is believed to have a tetrameric conformation similar to  $I_{Kr}$  channels, with S4 as a voltage sensor.  $I_{Ks}$  has a motif generally seen in other potassium channels in the S6 segment, proline-X-proline, which is thought to play a role in gating. S6 contains the alanine hinge, a residue that could favor maintenance of the  $\alpha$ -helical structure.<sup>14</sup> To form a functional  $I_{Ks}$  channel, *KCNQ1* requires coexpression of an accessory subunit (called *MinK*) encoded by *KCNE1*,<sup>15,16</sup> although the stoichiometry between the 2 molecules remains unknown.

*KCNA5* encodes the  $\alpha$ -subunit of the  $I_{Kur}$  channel, and its loss-of-function mutations have been shown to be associated with familial AF.<sup>17–19</sup> *Kv4.3* encodes the  $\alpha$ -subunit of  $I_{to,f}$  and can form multimeric tetramers with other Kv4.x channels, which produces a functional diversity of transient outward currents. As with *KCNQ1* and *KCNE1*, an increasing number of accessory subunits have been shown to modulate the expression and kinetics of Kv4.x channels: (1) Potassium channel-interacting proteins (*KChIPs*)<sup>20</sup>; (2) a calcium-binding protein, *NCS-1* (or frequenin)<sup>21</sup>; (3) potassium channel accessory proteins (*KChAPs*); (4) dipeptidyl-aminopeptidase-like protein 6 (*DPP6*); and (5) *KCNE* family members.<sup>22–25</sup> *KCNE* members are also denoted as *MinK*-related proteins (*MirP1* through 4, encoded by *KCNE2* through 5, respectively), and *KCNE2* (or *MirP1*) has been shown to modulate *KCNH2*-encoded  $I_{Kr}$  channels.<sup>26,27</sup> In addition, *MinK* also affects the  $I_{Kr}$  current.<sup>28–30</sup>

The *KCNJ* family consists of more than 10 members that encode inward-rectifying potassium channels; they have only 2 transmembrane segments (M1 and M2) and lack the voltage sensor. *KCNJ2* encodes  $I_{K1}$  channels (Kir2.1), which are abundantly expressed in heart and determine the resting membrane potential and final phase of action potential repolarization.<sup>31,32</sup> Another member of the *KCNJ* family, *KCNJ5*, encodes the  $\alpha$ -subunit of the acetylcholine-sensitive potassium current ( $I_{K-ACh}$ ) channel, which is opened by extracellular acetylcholine via activation of membrane G proteins. *KCNJ5* can collaborate with *KCNJ3* to form a highly active heteromultimer or can form a low to moderately active homomultimer.<sup>33</sup> *KCNJ8* is another gene that encodes an inward-rectifier potassium channel, Kir6.1, which is sensitive to intracellular ATP, ie, ATP-sensitive potassium ( $K_{ATP}$ ) channels.<sup>34,35</sup> In physiological conditions, Kir6.1 requires the sulfonylurea receptor to function as a membrane metabolic-electric receptor, and it develops a sensitivity to sulfonylurea drugs.<sup>36</sup> Kir6.1 is abundantly expressed in heart, and its activation during myocardial ischemia may contribute to shortening of the action potential duration (APD) and ischemia-related ST-segment elevation in the ECG. Recently, a gain-of-function mutation of *KCNJ8* was identified in a patient with idiopathic ventricular fibrillation (VF), which indicates that the mutation can cause the channel to open constitutively without ischemia.

Intracellular magnesium ions and membrane polyamines are naturally occurring blockers that induce a strong rectifying property, one of the common characteristics of inward-rectifying potassium channels.<sup>37–41</sup> In humans, Kir2.1 is expressed not only in the myocardium but also in brain and skeletal muscle.<sup>32</sup> Loss-of-function *KCNJ2* mutations display cardiac and extracardiac phenotypes known as Andersen-Tawil syndrome (LQT7). Moreover, specific mutations in the *KCNJ2* gene have been shown to be associated with variable phenotypes, such as catecholaminergic polymorphic ventricular tachycardia (VT), SQTS, and AF.

### Clinical Phenotype Due to Potassium Channel Gene Mutations, Including Genotype-Phenotype Correlations

Genotype-phenotype correlations have been investigated extensively in some inherited arrhythmia syndromes, and the

possibility of gene-specific risk stratification and gene-specific therapy and management has been suggested.

### Congenital LQTS

Congenital LQTS is characterized by a prolonged QT interval in the ECG and a polymorphic VT known as torsade de pointes.<sup>42,43</sup> Congenital LQTS is a Rosetta stone for studying the genetic background of inherited arrhythmic syndromes,<sup>6</sup> because multiple genes that encode the many different ion channels or membrane adaptor have been identified.

#### Genetics in Congenital LQTS

Since the first 3 genes responsible for the 3 major genotypes (LQT1, LQT2, and LQT3) were identified in the mid-1990s,<sup>3,4,44</sup> a total of 13 forms of Romano-Ward-type congenital LQTS have been reported to be caused by mutations in genes of potassium, sodium, and calcium channels or the membrane adaptor located on chromosomes 3, 4, 7, 11, 12, 17, 20, and 21.<sup>45–54</sup> Of the 13 identified genotypes, 6 (LQT1, LQT2, LQT5, LQT6, LQT7, and LQT13) are caused by mutations in potassium channel genes; in LQT11, *AKAP-9* encoding Yotiao is the responsible gene<sup>51</sup> (Table). *AKAP-9* is reported to assemble *KCNQ1*, thus indirectly modulating  $I_{Ks}$ . Mutations in *KCNQ1* and *KCNE1*, which are the  $\alpha$ -subunit and accessory subunit of the potassium channel gene, respectively, are responsible for defects (loss of function) in the  $I_{Ks}$  underlying LQT1 and LQT5.<sup>15,16</sup> Mutations in *KCNH2* and *KCNE2*, which are also the potassium channel  $\alpha$ -subunit and accessory subunit, respectively, cause defects in  $I_{Kr}$  that are responsible for LQT2 and LQT6.<sup>4,26</sup>; however, there is controversy as to whether  $I_{Kr}$  is truly the byproduct of *KCNH2* and *KCNE2*. Mutations in *KCNJ2* encoding  $I_{K1}$  underlie Andersen-Tawil syndrome (LQT7), in which QT prolongation and ventricular arrhythmias are accompanied by potassium-sensitive periodic paralysis and dysmorphic features that include low-set ears, hypertelorism, cleft palate, micrognathia, scoliosis, short stature, and syndactyly.<sup>46,55</sup> A specific *KCNJ2* mutation, V227F, was identified in a patient with a typical catecholaminergic polymorphic VT phenotype.<sup>56</sup> Heterologous expression with the COS cell line showed that heterozygous wild-type/V227F channels were identical to wild-type channels in function, but stimulation by cAMP-dependent protein kinase A significantly downregulated heterozygous mutant Kir2.1 and not wild-type Kir2.1 currents.<sup>56</sup> This particular type of loss of function explained why the proband displayed the catecholaminergic polymorphic VT phenotype, in which typical bidirectional or polymorphic VT is provoked by exercise. Most recently, a mutation in *KCNJ5* was reported to result in a loss of function of  $I_{K-ACh}$  responsible for LQT13,<sup>54</sup> although the precise role of  $I_{K-ACh}$  in the ventricle is still unknown. In all genotypes, decreases in outward potassium currents ( $I_{Ks}$ ,  $I_{Kr}$ ,  $I_{K1}$ , and  $I_{K-ACh}$ ) prolong the APD, which results in prolongation of the QT interval, a common phenotype. Prolongation of the action potential plateau phase allows recovery from inactivation and reactivation of L-type calcium channels, which produces early afterdepolarizations. The early afterdepolarization-induced ventricular premature contractions capture the vulnerable window created by increased transmural and spatial

dispersion of ventricular repolarization, thus resulting in torsade de pointes. In LQT7, loss of function in  $I_{K1}$ , which is active during the terminal phase of the action potential, prolongs the terminal repolarization phase and produces delayed afterdepolarization, which triggers typical multifocal or bidirectional VT.

The LQT1 and LQT2 syndromes are the 2 most common genetic variants, and each accounts for approximately 40% of genotyped patients.<sup>45</sup> The third most common genotype, LQT3, accounts for only 10% of genotyped patients.<sup>45</sup> Therefore, more than 80% of genotyped LQTS patients have potassium channel gene-related LQTS genotypes, which suggests that congenital LQTS is most frequently a disease of potassium channels.

Autosomal-recessive forms of Jervell and Lange-Nielsen syndrome are associated with neurosensorial deafness and generally more severe phenotype (marked QT prolongation and lethal ventricular arrhythmias) than autosomal-dominant forms of the Romano-Ward syndrome.<sup>57</sup> Two genotypes, JLN1 and JLN2, are reported to be responsible for homozygous or compound heterozygous mutations in the *KCNQ1* or *KCNE1* genes, and both are responsible for a decrease in  $I_{Ks}$ .

Congenital LQTS is believed to cause at least some cases of sudden infant death syndrome.<sup>58</sup> Mutations in *KCNQ1*<sup>59</sup> and *KCNHZ*<sup>59</sup> have been reported to be associated with sudden infant death syndrome.

#### Genotype-Phenotype Correlations in LQTS

##### ECG Characteristics

In the 3 major genotypes (LQT1, LQT2, and LQT3), a genotype-specific T-wave morphology in the 12-lead ECG was proposed by Moss and coworkers in 1995.<sup>60</sup> Broad-based prolonged T waves are more commonly observed in LQT1 with an  $I_{Ks}$  defect, whereas low-amplitude T waves with a notched or bifurcated configuration are more frequently observed in LQT2 with an  $I_{Kr}$  defect. Exercise treadmill testing has been reported to unmask the characteristic T-wave morphology in patients with LQT1 (broad-based T waves) or LQT2 (notched T waves).<sup>61</sup> In LQT7 with an  $I_{K1}$  defect, mild QT prolongation, TU-wave abnormalities (featuring a prominent U wave), frequent ventricular premature contractions, and typical bidirectional VT are often observed.<sup>46</sup>

A series of experimental studies that used arterially perfused canine wedge preparations developed in the late 1990s have delineated the cellular basis for the T-wave morphology that is characteristic of LQT1, LQT2, and LQT7.<sup>62–65</sup> The amplified transmural electric heterogeneity of ventricular repolarization associated with differential modification of potassium currents in each cell type, which is caused by mutations in each genotype, results in genotype-specific T-wave morphology in the ECG.<sup>62,63</sup> In the LQT1 model, preferential prolongation of the APD in midmyocardial (M) cells compared with epicardial and endocardial cells with an  $I_{Ks}$  blocker, chromanol 293B, and additional isoproterenol, a  $\beta$ -adrenergic agonist, creates a dramatic augmentation of transmural dispersion of repolarization, which results in broad-based T waves (Figures 1B and 1E).<sup>63,64</sup> In the LQT2 model, d-sotalol, an  $I_{Kr}$  blocker, in the presence of hypokalemia also produces more preferential APD prolongation in

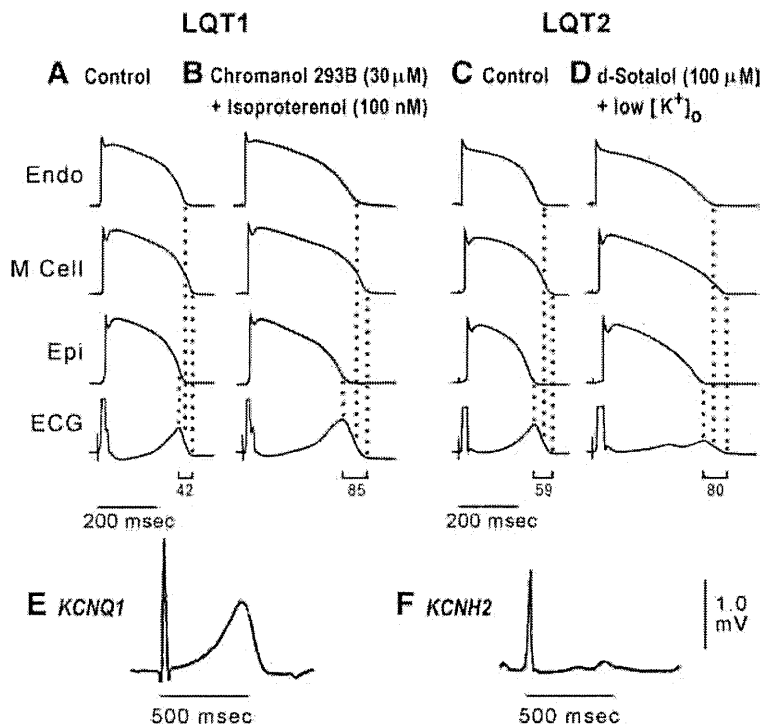


**Figure 1. Cellular basis of abnormal T-wave patterns in potassium channel gene-related LQT1 and LQT2 syndrome.** A through D, Transmembrane action potentials recorded simultaneously from endocardial (Endo), midmyocardial (M), and epicardial (Epi) cells together with a transmural ECG at a basic cycle length of 2000 ms in the LQT1 and LQT2 models of arterially perfused canine wedge preparations. E and F, ECG lead V<sub>5</sub> recorded in patients with LQT1 and LQT2 forms of congenital LQTS. Pharmacological models mimic the phenotypic appearance of the abnormal T waves in both models. Modified from Shimizu et al<sup>62,63</sup> with permission.

M cells and slowing of phase 3 of the action potential in all 3 cell types, which results in large transmural dispersion of repolarization and a low-amplitude T wave with the notched or bifurcated appearance characteristic of LQT2 (Figures 1D and 1F).<sup>62,64</sup> In the LQT7 model, cesium chloride, an I<sub>K1</sub> blocker, and isoproterenol delay late phase 3 repolarization of the action potential and induce delayed afterdepolarizations, which generates U waves and delayed afterdepolarization-induced ventricular premature contractions. Migration of delayed afterdepolarization foci is reported to be the mechanism that produces multifocal VT and characteristic bidirectional VT.<sup>65</sup>

#### Clinical Course

The cumulative probability of cardiac events (syncope, aborted cardiac arrest, sudden cardiac death) is higher in patients with the potassium channel gene-related LQTS genotypes (LQT1 and LQT2) than in patients with LQT3, a sodium channel gene-related LQTS genotype.<sup>66</sup> On the other hand, Priori and coworkers<sup>67</sup> reported that in more homogeneous LQTS cohorts, LQT1 was the variant associated with higher incomplete penetrance, and the event rate was significantly higher in LQT2 (46%) and LQT3 (42%) than in LQT1 (30%). Some evidence points to more severe arrhythmia consequences of *SCN5A* mutations.<sup>68</sup> In general, male patients experience their first cardiac events at a younger age than female patients.<sup>69</sup> Approximately 90% of first cardiac events occur before the age of 15 years in male patients, particularly in males with LQT1, whereas female patients rarely experience their first cardiac event occasionally after the age of 20 years.<sup>67,69</sup> A recent large cohort of patients with LQT1 and LQT2 syndromes confirmed these tendencies and suggested that age younger than 13 years combined with male gender and age older than 13 years combined with female

gender were significant and independent clinical risk factors associated with first cardiac events in both LQT1 and LQT2 syndromes.<sup>70,71</sup>

#### Genotype-Specific Triggers for Cardiac Events

Triggers for LQTS-related cardiac events have been reported to differ between each LQTS genotype, including LQT1, LQT2, and LQT7.<sup>43,72,73</sup> Although sympathetic stimulation may trigger cardiac events in all potassium channel gene-related LQTS genotypes, LQT1 with the I<sub>Ks</sub> defect is the most sensitive to sympathetic stimulation. Cardiac events in LQT1 patients most frequently occur during exercise (62%), and swimming is a common trigger.<sup>72</sup> LQT2 is less likely to result in cardiac events during exercise (13%) and more likely to result in cardiac events during rest or sleep (29%).<sup>72</sup> More specifically, being startled by an auditory stimulus (telephone, alarm clock, ambulance siren, etc) is a specific trigger in LQT2.<sup>72,73</sup> Women with LQT2 are reported to be the most susceptible to cardiac events during the postpartum period.<sup>74</sup> Both experimental studies using arterially perfused wedge preparations<sup>63,64</sup> and clinical studies using catecholamine provocative testing or exercise testing<sup>61,75-78</sup> have suggested that the differential sensitivity of cardiac events in each genotype (LQT1, LQT2, and LQT3) in response to sympathetic (β-adrenergic) stimulation is due to the differential response of ventricular repolarization to sympathetic stimulation. In LQT7 patients, hypokalemia is often associated with frequent ventricular arrhythmias and periodic paralysis<sup>46</sup>; however, periodic paralysis is also associated with hyperkalemia or normokalemia.<sup>46</sup>

#### Diagnostic Value of Epinephrine Challenge Test

It is well known that some genetically affected LQTS patients may have a normal or borderline QT interval but harbor a



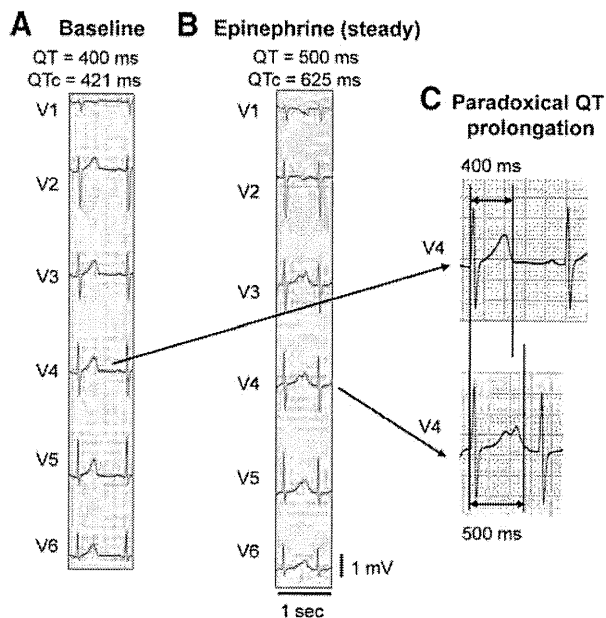


**Figure 2. Paradoxical QT prolongation during epinephrine challenge test in a patient with LQT1 syndrome.** Shown are 6 precordial ECG leads under baseline conditions and at steady state after epinephrine. The QTc interval was remarkably prolonged from 421 to 625 ms at steady state. Absolute QT interval was also prolonged from 400 to 500 ms, even though the RR interval was apparently abbreviated (paradoxical QT prolongation).

lethal arrhythmogenic substrate.<sup>67,79</sup> This fact strongly points to the need for new diagnostic tools to unveil concealed forms of LQTS. Recent major insights have been gleaned using epinephrine, an  $\alpha$ - and  $\beta$ -adrenergic agonist, as a provocative test.<sup>75–78</sup> The 2 major protocols developed for the epinephrine challenge test include the escalating-dose protocol by Ackerman's group (Mayo protocol)<sup>77,78</sup> and a bolus injection followed by a brief continuous infusion by our group (Shimizu protocol).<sup>75,76,78</sup>

Ackerman and coworkers<sup>77</sup> reported that paradoxical QT prolongation had a sensitivity of 92.5%, a specificity of 86%, a positive predictive value of 76%, and a negative predictive value of 96% for LQT1 patients versus non-LQT1 patients (Figure 2). Our bolus protocol, which was developed on the basis of data from experimental LQTS models,<sup>64</sup> suggested that sympathetic stimulation produces genotype-specific responses of the corrected QT (QTc) interval in patients with LQT1, LQT2, and LQT3 syndromes.<sup>75,76,78</sup> The bolus protocol of epinephrine improves clinical ECG diagnosis (sensitivity) in patients with either LQT1 or LQT2 with a potassium channel defect but not in patients with LQT3 with a sodium channel defect.<sup>76</sup> The bolus protocol also effectively predicts the underlying genotype of LQT1, LQT2, and LQT3.<sup>76,78</sup> A presumptive, pregenetic diagnosis of either LQT1, LQT2, or LQT3 based on the response to an epinephrine challenge test can facilitate the molecular genetic diagnosis by targeting a first candidate gene and can guide genotype-specific treatment strategies.<sup>78</sup> Although epinephrine was not used, Viskin et al<sup>80</sup> recently reported the usefulness of a bedside stand-up test to easily diagnose LQTS. They suggested that at maximal

QT-interval stretching, the time at which the end of the T wave is nearest to the next P wave during transient sinus tachycardia after a person stands up quickly, the QTc value identifies LQTS with 90% sensitivity and 86% specificity.<sup>80</sup>

#### Genotype-Specific Patient Care and Therapy

Because LQT1 patients are most sensitive to sympathetic stimulation, and most of their first cardiac events occur before the age of 15 years, particularly in males with LQT1 syndrome, strict exercise restriction, particularly restriction of swimming, diving, or competitive sports, is needed in these patients.<sup>81</sup> Exercise restriction is also required in LQT2 patients.<sup>81</sup> In LQT2, the avoidance of specific acoustic triggers, such as alarm clocks and a ringing telephone, is required and effective. It is also important to instruct elderly patients with LQT1 and LQT2 to avoid QT-prolonging agents, hypokalemia, and bradycardia.

Genotype-specific pharmacological and nonpharmacological therapies have been introduced clinically on the basis of data derived from both clinical and experimental studies.<sup>81</sup> In LQT1,  $\beta$ -blockers are most effective to prevent episodes of syncope and sudden cardiac death.<sup>70,72,82</sup> The largest international cohort of 600 LQT1 patients suggested that time-dependent  $\beta$ -blocker use was associated with a significant 74% reduction in the risk of first cardiac events.<sup>70</sup> Mexiletine, a class IB sodium channel blocker that blocks late  $I_{Na}$ , or verapamil, an  $I_{Ca-L}$  blocker, may warrant consideration as adjunctive therapy to  $\beta$ -blockers in LQT1 patients.<sup>62,63</sup> As a nonpharmacological therapy, left stellate ganglion ablation, another antiadrenergic therapy, is most effective in LQT1 patients.<sup>83</sup> An implantable cardioverter-defibrillator is indicated for LQTS patients who have experienced an aborted cardiac arrest or who have repetitive episodes of syncope in the presence of  $\beta$ -blockers.

In LQT2,  $\beta$ -blockers are also effective; however, previous studies have suggested that the effectiveness of  $\beta$ -blockers is somewhat less in either LQT2 or LQT3 patients than in LQT1 patients.<sup>72,84</sup> Priori et al<sup>84</sup> reported that cardiac events among patients receiving  $\beta$ -blocker therapy occurred in 10% of LQT1 patients, 23% of LQT2 patients, and 32% of LQT3 patients. A report on a recent international cohort of 858 LQT2 patients suggested that time-dependent  $\beta$ -blocker use significantly reduced the risk of first cardiac events by 63%, which confirms the efficacy of  $\beta$ -blockers as a first-line therapy in LQT2.<sup>71</sup> Maintenance of the extracellular potassium concentration by long-term oral potassium supplementation is reported to be effective because it shortens the QT interval in LQT2 patients.<sup>85</sup> A genotype-specific initiating pattern of torsade de pointes has been reported.<sup>86,87</sup> A characteristic short-long-short initiating pattern of torsade de pointes, which is frequently observed in drug-induced torsade de pointes in acquired LQTS, is more frequently seen in LQT2 and LQT3 patients than in LQT1 patients.<sup>87</sup> Therefore, pacemaker therapy is expected to be more effective in LQT2 than in LQT1 patients via suppression of the specific short-long-short initiating pattern.<sup>87</sup> The indication for implantable cardioverter-defibrillator is similar to that in LQT1 syndrome.

There is no known genotype-specific therapy for other potassium channel gene-related LQTS genotypes (LQT5,

LQT6, LQT7, LQT11, and LQT13), in which  $\beta$ -blockers may be the first-line therapy.

#### **Mutation Site-Specific Risk Stratification and Therapy**

As the correspondence between the mutation site and the cardiac potassium channel and the structure of the potassium channel have become increasingly discovered, mutation site-specific risk stratification or therapy can be expected in potassium channel gene-related LQTS. In 2004, Shimizu and coworkers<sup>88</sup> compared the arrhythmic risk and sensitivity to sympathetic stimulation with treadmill exercise testing between Japanese LQT1 patients with transmembrane mutations and those with C-terminal mutations in the *KCNQ1* gene. The LQT1 patients with transmembrane mutations had a longer QTc and more frequent cardiac events than those with C-terminal mutations.<sup>88</sup> Moreover, the QTc prolongation with exercise was more remarkable in the LQT1 patients with transmembrane mutations.<sup>88</sup> The more severe phenotype in LQT1 patients with transmembrane mutations was confirmed later in a much larger international cohort that consisted of 600 LQT1 patients.<sup>70</sup> Results from that cohort also suggested that LQT1 patients with mutations that had dominant-negative (>50%) ion channel effects were at greater risk for cardiac events than those who had haploinsufficiency ( $\leq$ 50%) ion channel effects. In 2002, Moss and coworkers<sup>89</sup> reported that LQT2 patients with mutations in the pore region of the *KCNH2* gene had a greater risk of arrhythmia-related cardiac events than those with nonpore mutations. A recent larger international cohort investigated the clinical aspects of 858 subjects with a spectrum of *KCNH2* mutations categorized by the distinct location, coding type, and topology of the channel mutations.<sup>71</sup> The LQT2 patients with *KCNH2* missense mutations located in the transmembrane S5-loop-S6 region were reported to be at greatest risk. In this cohort, a significantly higher risk was found in the LQT2 patients with mutations located in the  $\alpha$ -helical domains than in those with mutations in the  $\beta$ -sheet domains or other locations.<sup>71</sup> These data indicate the possibility of mutation site-specific management or treatment in patients with potassium channel gene-related LQTS.

#### **Short-QT Syndrome**

SQTS is characterized by an abnormally short QT interval and increased risk of VF and sudden death.<sup>90,91</sup> In 2000, Gussak and coworkers<sup>90</sup> reported a first case with SQTS who showed a short QTc of 300 ms and AF. In 2003, Gaita et al<sup>91</sup> described 2 families with SQTS associated with a family history of sudden cardiac death due to malignant ventricular arrhythmias. Thereafter, increasing attention has been given to SQTS; however, the number of SQTS patients is still very limited. No clinically diagnostic criteria have been described, and a short QTc is generally considered as  $\leq$ 300 to 320 ms.<sup>90,91</sup> The diagnosis of SQTS was made if a patient with QTc  $\leq$ 330 ms had an arrhythmic event, including documented VF, resuscitated sudden cardiac death, and syncope; and/or a family history of SQTS; or if a patient with QTc  $\leq$ 360 ms had mutations in the ion channel genes responsible for SQTS.<sup>92,93</sup>

#### **Genetics in SQTS**

Five genotypes have been identified in SQTS to date (Table), of which the SQT1, SQT2, and SQT3 genotypes are caused by mutations in genes that encode the potassium channel (*KCNH2*, *KCNQ1*, and *KCNJ2*, respectively).<sup>94–96</sup> *KCNH2*, *KCNQ1*, and *KCNJ2* are potassium genes responsible for the LQT2, LQT1, and LQT7 types of congenital LQTS, but all mutations reported in these 3 potassium genes biophysically demonstrate gain of function of  $I_{Kr}$ ,  $I_{Ks}$ , and  $I_{K1}$ , respectively, thus shortening the APD and the QT interval.

#### **Genotype-Phenotype Correlations in SQTS**

In addition to a short QT interval, genotype-specific T-wave morphology in the 12-lead ECG has been reported in the potassium channel gene-related SQTS genotypes (SQT1, SQT2, and SQT3).<sup>94–96</sup> In SQT1, the T waves in the precordial leads are reported to be symmetrical and tall,<sup>94</sup> but the  $T_{peak}$  to  $T_{end}$  interval, which reflects transmural dispersion of repolarization, is relatively prolonged, and this is suggested to produce a substrate for reentry that leads to VF.<sup>97</sup> The T waves are symmetrical but not as tall in SQT2.<sup>95</sup> In contrast, the T waves in SQT3 illustrate an asymmetrical pattern, with a less steep ascending part of the T wave followed by an accelerated descending T wave.<sup>96</sup> The rapid descending terminal phase of the T waves can be explained by an accelerated terminal phase of repolarization due to gain of function of  $I_{K1}$ .<sup>96</sup>

A recent clinical study reported a high prevalence of early repolarization in patients with SQTS associated with arrhythmic events.<sup>98</sup> An implantable cardioverter-defibrillator is the most reliable therapy for secondary prevention in SQTS patients with a history of VF or aborted sudden cardiac death. As an adjunctive medication, quinidine has been reported to normalize the QT interval and T-wave morphology and to suppress the induction of VF during electrophysiological study in patients with SQT1<sup>99</sup>; however, it is not clear whether the specific efficacy of quinidine observed in SQT1 patients was genotype specific or mutation specific.

#### **Brugada Syndrome**

BrS is characterized by coved-type ST-segment elevation (type 1) in the right precordial ECG (leads  $V_1$  through  $V_3$ ) and an episode of VF in the absence of structural heart diseases.<sup>100–103</sup> The prevalence of BrS is estimated to be up to 5 per 10 000 persons, and BrS is one of the important causes of sudden cardiac death of middle-aged males, particularly in Asian countries.<sup>102,103</sup> BrS usually manifests during adulthood,<sup>102</sup> and more than 80% to 90% of patients clinically affected with BrS are men.

#### **Genetics in BrS**

Since the first mutation linked to BrS was identified in *SCN5A*, the  $I_{Na}$  gene, in 1998,<sup>104</sup> which presently accounts for 11% to 28% of patients with clinically diagnosed BrS,<sup>105</sup> 7 responsible genes have been reported. In all 7 genotypes, either a decrease in the inward sodium or calcium current or an increase in the outward potassium current is responsible for the Brugada phenotype; however, approximately two thirds of Brugada patients have not yet been genotyped, which suggests the presence of genetic heterogeneity.<sup>103</sup>

There is only 1 potassium channel gene among the 7 genes responsible for BrS (Table). Delpón et al<sup>23</sup> reported a missense mutation (R99H) in *KCNE3*, which encodes the potassium channel accessory ( $\beta$ 3) subunit and interacts with the *Kv4.3* ( $I_{to}$ ) channel, in a proband with BrS. Coexpression of the mutant *KCNE3* with *KCND3*, which encodes *Kv4.3*, increases  $I_{to}$  intensity (gain of function) compared with coexpression of wild-type *KCNE3* with *KCND3*.<sup>23</sup> We recently reported that *KCNE2* and *KCNE5*, auxiliary potassium channel accessory subunits, are other genes responsible for potassium channel gene-related BrS via the modulating effect of the  $I_{to}$ .<sup>24,25</sup>

#### Genotype-Phenotype Correlations in BrS

The genotype-phenotype correlation in BrS has been less investigated than that in congenital LQTS and is limited in sodium channel gene (*SCN5A*)-related BrS. None of the conduction abnormalities that have been reported in patients with *SCN5A*-related BrS (such as widening of the P wave, prolongation of QRS duration, PQ interval, or right bundle-branch block) were described in the patient with potassium channel gene-related BrS6 reported by Delpón et al.<sup>23</sup> Several agents that increase the outward potassium current, such as nicorandil, a  $K_{ATP}$  channel opener, have the potential to induce transient ST-segment elevation like that in BrS and have been described as an "acquired" form of BrS.<sup>102,106</sup>

#### Early Repolarization Syndrome

The prevalence of an early repolarization pattern or J wave in the inferior (II, III, aVF) or lateral (I, aVL,  $V_4$  through  $V_6$ ) leads is estimated to be 1% to 5% of healthy individuals, and these had been considered benign ECG characteristics.<sup>107</sup> However, several reports have focused increasing attention on the association of idiopathic VF with early repolarization in the inferior or lateral leads, so-called early repolarization syndrome. Haissaguerre et al<sup>108</sup> reported that early repolarization was more frequently recognized in idiopathic VF patients than in control subjects, and they reported a higher incidence of VF recurrence in case subjects with early repolarization than in those without.

#### Genetics in Early Repolarization Syndrome

A novel missense mutation, S422L, in the *KCNJ8*-encoded Kir6.1  $\alpha$ -subunit of the  $K_{ATP}$  channel was reported in a young female with VF secondary to early repolarization syndrome.<sup>109</sup> A recent study reported that the  $K_{ATP}$  current ( $I_{K-ATP}$ ) of the Kir6.1-S422L mutation was increased significantly (gain of function), thus promoting an early repolarization pattern or J wave in the ECG.<sup>110</sup> (See Table.)

#### Genotype-Phenotype Correlations in Early Repolarization Syndrome

No studies showing a genotype-phenotype correlation have been reported in early repolarization syndrome.

#### Atrial Fibrillation

AF is the most commonly observed cardiac arrhythmia encountered in clinical practice. AF is usually accompanied by organic heart diseases such as valvular heart disease, hypertensive heart disease, or hypertrophic or dilated cardiomyopathy; however, AF without organic heart disease (lone

AF) also occurs. Some genetic factors or genetic backgrounds that predispose to AF may be linked to the development of AF, especially in familial forms of AF, in which the AF is segregated in several family members.

#### Genetics in AF

The epidemiological data have suggested that the relative risk of AF in offspring was increased significantly if parents had AF before 60 years of age,<sup>111</sup> which indicates heritability in AF. There are 3 categories of genetic patterns related to AF: (1) familial AF as a monogenic disease; (2) familial AF associated with other inherited cardiac diseases, including hypertrophic cardiomyopathy, dilated cardiomyopathy, and skeletal myopathies or other inherited arrhythmic syndromes, including congenital LQTS, SQTs, and BrS; and (3) nonfamilial AF associated with genetic backgrounds that predispose to AF, such as a polymorphism in the angiotensin-converting enzyme gene (*ACE*). Mutations in several potassium channel genes have been reported to be responsible for AF; however, all mutations reported thus far were identified in isolated patients or families.

The first mutation linked to AF was identified in *KCNQ1*, the  $I_{Ks}$  gene, in 2003<sup>112</sup> (Table). Electrophysiological analysis of the specific mutation, S140G, demonstrated a gain of function in  $I_{Ks}$  current, which results in shortening of the APD and effective refractory period in the atrium, providing the substrate for AF. The same scenario was expected in the ventricle, leading to abbreviation of the QT interval, but 9 of the 16 affected individuals presented with QT prolongation, which could not be well explained. Thereafter, mutations in *KCNE2* and *KCNE3*, which are both accessory subunits, were found in familial AF.<sup>113,114</sup> Although the *KCNE2* mutation (R27C) coexpressed with *KCNQ1* resulted in a gain of function of  $I_{Ks}$ , the *KCNE3* mutation (R53H) did not change  $I_{Ks}$ , which suggests that it might not be a causative mutation. A *KCNJ2* mutation that leads to a gain of function in  $I_{K1}$  current has also been reported.<sup>115</sup> More recently, a mutation in *KCNA5* encoding an atrium-specific  $I_{Kur}$  was identified in familial AF.<sup>17-19</sup> Interestingly, the specific *KCNA5* nonsense mutation E375X resulted in a loss of function of  $I_{Kur}$  current. A reduction in  $I_{Kur}$  elevates the voltage of the action potential plateau, thus activating more  $I_{Kr}$  and enhancing atrial repolarization. The resultant APD abbreviation is believed to create the substrate for AF.<sup>116</sup> The specific *KCNH2* mutation N588K has been reported to produce an overlap phenotype of familial AF and the SQT1 form of SQTs.<sup>117</sup> One specific mutation in the natriuretic peptide precursor A gene (*NPPA*) that encodes atrial natriuretic peptide has been reported recently to indirectly increase the  $I_{Ks}$  current, which results in shortening of the atrial APD.<sup>118</sup>

#### Genotype-Phenotype Correlations in AF

No studies showing genotype-phenotype correlations have been reported in AF.

#### Diverse Mechanisms Underlie the Generation of Cardiac Potassium Channel Diseases

According to the central dogma of molecular biology (Figure 3, steps 1 through 10), it is now accepted that several steps lead to channel dysfunction: A genetic variant (step 1 in

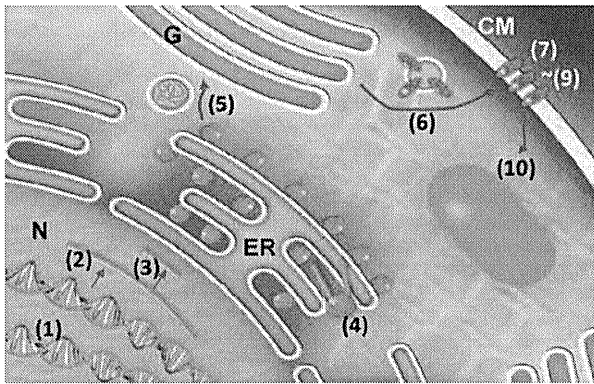


**Figure 3. Scheme showing the central dogma of protein synthesis.** Numbers in parentheses (1 through 10) in the cartoon indicate diverse mechanisms underlying cardiac potassium channel diseases. For detailed explanation, see text. ER indicates endoplasmic reticulum; CM, cardiac cell membrane; G, Golgi apparatus; and N, cellular nucleus.

Figure 3) impairs transcription (step 2), splicing and related processes (step 3), and translation (step 4).<sup>119–122</sup> With regard to the genetic variants, 3 categories are associated with cardiac potassium channel diseases: mutations, single-nucleotide polymorphisms, and copy-number variations. The former 2 are usually involved in single-nucleotide replacement or insertion/deletion. A variety of mutations in the potassium channel or its related genes have been shown to cause disease by affecting every step shown in Figure 3 (steps 2 through 10). Among the single-nucleotide polymorphisms involved in potassium channel diseases, *KCNE1* D85N is well known not only as a modifier but also as a causative variant of LQTS.<sup>30,123</sup> In contrast, copy-number variations contain relatively large regions of the genome (kilobases to several megabases), with deletion (fewer than the normal number) or duplication (more than the normal number) on a certain chromosome, thereby giving the genome diversity. Recently, several copy-number variations in *KCNH2* and *KCNQ1* have been shown to be associated with disease.<sup>124–126</sup> More recently, a French group conducted an extensive survey of copy-number variations in *KCNQ1* and *KCNH2* and demonstrated that such variations explained approximately 3% of LQTS in patients with no point mutation in these genes.<sup>127</sup>

With regard to the posttranslational process, impaired intracellular transport (steps 5 and 6 in Figure 3) is a common cause of LQTS in several *KCNQ1*, *KCNJ2*, and most *KCNH2* mutations.<sup>128–132</sup> *KCNJ2* contains a specific C-terminal sequence necessary for exportation from the endoplasmic reticulum to the Golgi apparatus (endoplasmic reticulum-to-Golgi export signal).<sup>133</sup> More recently, a naturally occurring *KCNJ2* mutation in the C terminus (S369X), located immediately upstream of this endoplasmic reticulum export signal, was shown to cause a limited form of Andersen-Tawil syndrome (LQT7) by impeding transportation from the endoplasmic reticulum to Golgi (step 5 in Figure 3).<sup>134</sup>

Most *KCNH2* mutations have been reported to reduce hERG currents by a trafficking-deficient mechanism (step 6 in Figure 3).<sup>131</sup> Several trafficking-refractory *KCNQ1* mutations are also known, of which T587M in the C-terminal region was the first reported.<sup>128</sup> The mutation produced a more severe

phenotype than expected by the results of functional analysis; the mutation produced no dominant-negative suppression effects on wild-type channels. This mysterious discrepancy was found to result from the physical interaction between *KCNQ1* and *hERG* proteins, which increased localization of hERG channels to the cell membrane, enhanced current density, and altered their biophysical properties.<sup>135</sup> Likewise, overexpression of the dominant-negative *KCNQ1* or *hERG* transgene in genetically modified rabbits resulted in downregulation of the remaining reciprocal current, which indicates that the 2 proteins indeed interact in vivo as well.<sup>136</sup> Therefore, the intracellular trafficking defect in *KCNQ1* impaired the physical interaction with *hERG* and thereby caused severe clinical features (step 6 in Figure 3).<sup>137</sup>

Even after successful expression in membrane, alterations in channel function (steps 7 through 9 in Figure 3) induced by mutations are also pathological: those in potassium permeation (step 7), voltage gating (step 8), and modulation by various physiological stimulations, including protein kinase A and membrane phosphoinositide phosphatidylinositol 4,5-bisphosphate (PIP2).<sup>51,56,138,139</sup> Finally, endocytosis of channel proteins (step 10 in Figure 3) regulates its degradation apart from the plasma membrane. More recently, cholesterol has been shown to regulate Kv1.5 channel expression by modulating its trafficking through the Rab11-associated recycling endosome.<sup>140</sup> Impaired endocytosis of calcium-activated nonselective cation channels, TRM4, was reported to cause progressive cardiac conduction block through *SUMO* (small ubiquitin modifier) conjugation.<sup>141,142</sup> Heat shock proteins have also been shown to regulate *hERG* expression. *hERG* channels with disease-causing missense mutations in intracellular domains had a higher binding capacity to Hsc70 than wild-type channels, and knockdown of Hsc70 by small interfering RNA prevented degradation of mutant proteins with these mutations.<sup>143</sup>

Such diverse mechanisms have been elucidated, mainly by use of a heterologous expression system in mammalian cell lines; however, a big missing link between genotype and phenotype correlations remains. The recent introduction of induced pluripotent stem cells derived from patients may offer a novel methodology for use in the research of ion channelopathies.<sup>144</sup>

### Sources of Funding

Drs Shimizu and Horie were supported by a health sciences research grant (H18, Research on Human Genome, 002) and a research grant for cardiovascular diseases (21C-8, 22-4-7) from the Ministry of Health, Labour, and Welfare, Japan. Dr Horie was also supported by research grants from the Ministry of Education, Culture, and Technology of Japan and the Uehara Memorial Foundation.

### Disclosures

None.

### References

1. Priori SG. The fifteen years of discoveries that shaped molecular electrophysiology: time for appraisal. *Circ Res*. 2010;107:451–456.
2. Keating M, Atkinson D, Dunn C, Timothy K, Vincent GM, Leppert M. Linkage of a cardiac arrhythmia, the long QT syndrome, and the Harvey ras-1 gene. *Science*. 1991;252:704–706.